

CHARACTERIZING VARIABILITY IN RAMAN SPECTROSCOPY FOR NON-INVASIVE
HYDRATION MONITORING

By

Anna Sue Rourke

Thesis

Submitted to the Faculty of the
Graduate School of Vanderbilt University
in partial fulfillment of the requirements

for the degree of

MASTER OF SCIENCE

In

Biomedical Engineering

May 12, 2023

Nashville, Tennessee

Approved:

Anita Mahadevan-Jansen, Ph.D.

Justin S. Baba, Ph.D.

ACKNOWLEDGMENTS

I would like to thank the funding source that made this work possible. The generous support from the US Army Medical Research and Development Command (W81XWH-20-2-0064) provided the equipment and supplies necessary for this work.

I would like to thank my advisor Dr. Anita Mahadevan-Jasen, who supported me and guided me through this work. I would also like to acknowledge Dr. Andrea Locke for her mentorship throughout my graduate work. I would like to thank all the members of the Vanderbilt Biophotonics Center for their help in this work and for their willingness to serve as participants in my research studies; this work could not have been completed without them. I would also like to give a special thanks to my current lab members: Sean Fitzgerald, Trevor Voss, Jacob Hardenburger, Parker Willmon, Ezekiel Haugen, and Han Dong, who have helped me numerous times and provided countless advice. I am especially thankful to the members of the Raman group for their advice and guidance when I was stuck on the various problems this project posed. I am also thankful to the lab alumni who helped me during my work: Dr. Wilson Adams, Dr. Graham Throckmorton, Dr. Laura Masson, and Dr. Laura Elstub. Laura Masson not only handed this project off to me but was an invaluable friend and mentor to me. She spent countless hours teaching and guiding me and I wouldn't be the researcher I am today without her. I would not have made it through this work without the support of Laura Elstub and am grateful each day for the time she spent in the group. She not only brought guidance and knowledge to the hydration project, but also was a friend who was by my side during the craziness of graduate school. Lastly, I would like to acknowledge Mayna Nguyen, whose friendship helped make graduate school a little more bearable. Without her friendship, I would not have been able to make it through these past couple of years.

Lastly, I would like to thank my family and my husband, Gavin, who have provided unconditional love, support, and encouragement during this work. I am especially thankful for Gavin's daily support, encouragement, advice, and knowledge and wouldn't be here today without him.

TABLE OF CONTENTS

ACKNOWLEDGMENTS	ii
LIST OF TABLES	iv
LIST OF FIGURES	v
CHAPTER 1: INTRODUCTION	1
Overview of Hydration and Dehydration	1
Methods for Assessing Hydration	4
Raman Spectroscopy	7
Previous Water Analysis with Raman Spectroscopy	8
Thesis Hypothesis	9
CHAPTER 2: RAMAN SPECTROSCOPY FOR NON-INVASIVE HYDRATION MONITORING: FEASIBILITY AND EVALUATION OF VARIABILITY	10
Abstract	10
Introduction	10
Methods	12
Raman spectroscopy system	12
Tissue-mimicking phantom validation	13
<i>In vivo</i> studies	13
Data processing and analysis	16
Statistical analysis	17
Results	18
Gelatin-based phantoms	18
Inter-subject variability	19
Optimal location	20
Exercise standardization	21
Hydration standards	21
Gender variation	22
Repetitive measurement variability	23
Discussion	24
Conclusion	30
CHAPTER 3: CONCLUSIONS AND FUTURE DIRECTIONS	31
Future Directions	31
REFERENCES	32

LIST OF TABLES

Table 1. Participant demographics for three <i>in vivo</i> studies.....	14
Table 2. Overview of exercise protocols utilized in each <i>in vivo</i> study.	15

LIST OF FIGURES

Figure 1. Feedback loop that regulates water balance in the body. Figure from Jéquier <i>et al.</i> , European Journal of Clinical Nutrition 2009. ⁴	1
Figure 2. Pathophysiology of cognitive effects from dehydration. Figure from Wilson <i>et al.</i> , European Journal of Clinical Nutrition, 2003. ¹⁵	3
Figure 3. Distribution of total body water (TBW) in the body. Figure from Garrett <i>et al.</i> , IEEE Rev Biomed Eng, 2017. ³¹	5
Figure 4. (A) Schematic of anti-Stokes, Stokes Raman scattering, and elastic scattering (Rayleigh scattering); (B) Jablonski diagram of scattering processes showing changes in energy levels. Figure from Liu <i>et al.</i> , <i>Front Bioeng Biotechnol</i> , 2022. ⁶⁰	7
Figure 5. Raman spectrum of pure water showing location and intensity of the FP and HW water features. Figure from Alinovi <i>et al.</i> <i>Foods</i> , 2020. ⁶	8
Figure 6. Diagram of fiber optic probe layout for System 1 (A) and System 2 (B). The red fiber represents the excitation fiber. The green fibers represent the inner fibers; blue fibers represent the middle fibers, and the purple fibers represent the outer fibers.....	13
Figure 7. ATAGO digital handheld refractometer used for uSG measurements. Figure adapted from ATAGO.com.....	16
Figure 8. Flowchart of Raman data processing protocols.....	17
Figure 9. Gelatin-based phantoms with varying water content.....	18
Figure 10. Water band AUC percent change for each location in Study 2.....	19
Figure 11. Analysis of inter-subject variability.....	20
Figure 12. Analysis of four measurement locations.....	20
Figure 13. Analysis of effect of exercise intensity and standardization.....	21
Figure 14. Clinical standard correlation.....	22
Figure 15. Analysis of gender effects.....	23
Figure 16. Inter-measurement variability in Study 3.....	24
Figure 17. Participant pre-exercise hydration.....	26

CHAPTER 1: INTRODUCTION

Overview of Hydration and Dehydration

Water makes up a substantial portion of the body and is essential for life. Water has various functions in the body including acting as a solvent and reactant for chemical processes, a carrier for nutrient and waste products, and plays mechanical roles of lubrication and shock absorption. Water is a fundamental building block of the human body as it is present in every cell and tissue in the body. Additionally, water has a function in all hydrolytic reactions that take place in the body. Finally, water in the body transports nutrients between cells, allows for adequate blood circulation, and transports waste out of the body¹⁻⁴. As the body is constantly losing water through the lungs, skin, and kidneys, we must continually intake water to maintain adequate hydration. Water is lost through urinary output, evaporation via the respiratory tract, and through perspiration⁵. Water balance is regulated by a complex feedback loop that triggers the thirst reflex (**Figure 1**). While this is a tightly controlled feedback loop to ensure adequate hydration of the body, thirst can disappear before water balance is regained.

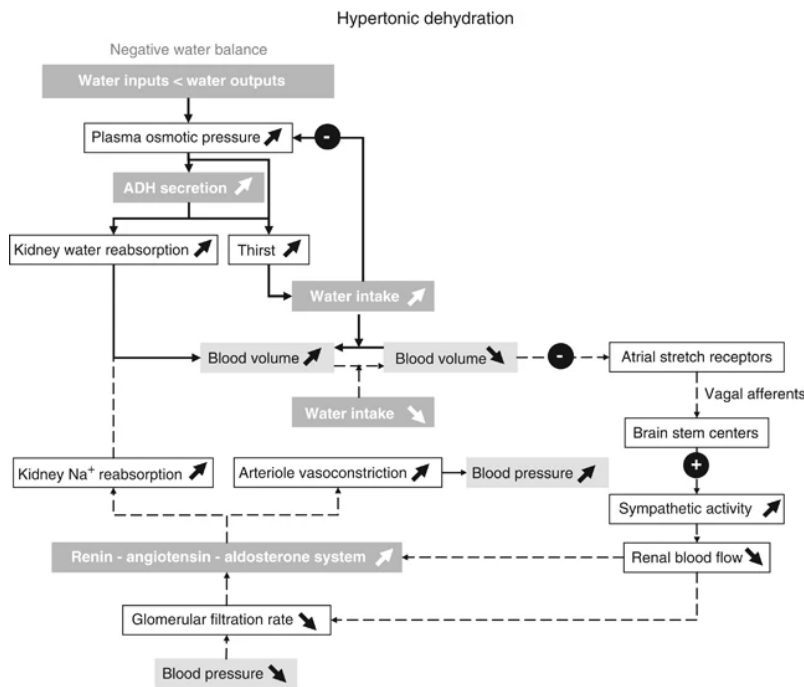


Figure 1. Feedback loop that regulates water balance in the body. Figure from Jéquier *et al.*, *European Journal of Clinical Nutrition* 2009.⁴

Due to the various biological processes that depend on water, dehydration can have severe negative effects, both physically and cognitively. Dehydration is a dynamic state and is defined as a loss in body water such that the water intake and loss is out of balance⁶. Dehydration impacts thermoregulation, the cardiovascular system, gastrointestinal system, urinary system, and integumentary system, as well as various other systems. The body's ability to regulate its temperature decreases as dehydration increases, thus increasing the core temperature of the body. Dehydration impairs heat loss, both dry and evaporative, delays the onset of sweating, and skin vasodilation⁷. The cardiovascular system is negatively affected by dehydration via significant reductions of blood volume, cardiac output, stroke volume, mean arterial pressure, and increased systemic vascular resistance and cutaneous vascular resistance^{8,9}. Gastric emptying and constipation are negatively affected by dehydration¹⁰⁻¹². Water has a crucial role in the filtering of waste from the blood stream in the kidneys and dehydration can decrease the efficiency of kidney filtration⁹. The integumentary system is negatively affected by water loss by reduced skin elasticity, skin thickness, and skin density^{9,13,14}. Dehydration has also been linked with certain chronic diseases such as urolithiasis and nephrolithiasis, chronic constipation, asthma, urinary tract infections, coronary heart disease, and cerebral infarction^{9,12}. Cognitively, dehydration can impair short- and long-term memory, impair reaction time, lead to acute confusion/delirium, and various other effects⁹. Cognitive effects are typically resultant of hypovolemia, or a reduction in plasma levels, and cerebral hypoperfusion caused by inadequate water intake¹⁵. While no operational definition of cognition exists, various working models to explain the effects of dehydration on cognition have been developed. One predominant theory, proposed by Cohen *et al.*, postulates that dehydration acts as a stressor and competes for executive attention and awareness, thereby reducing the overall cognitive performance¹⁶. Pathophysiological responses to dehydration have been observed including hypercortisolemia, elevated cerebral arginine vasopressin and nitric oxide synthase release, mitochondrial dysfunction, and increased secretion of cytokines (**Figure 2**). Three regions of the brain have also been identified as being the most vulnerable to the effects of dehydration: the reticular activating system, the autonomic structures, and the mid-brain structures. These regions are responsible for attention, wakefulness, regulating psychomotor and regulatory functions, and thought, memory, and perception¹⁷.

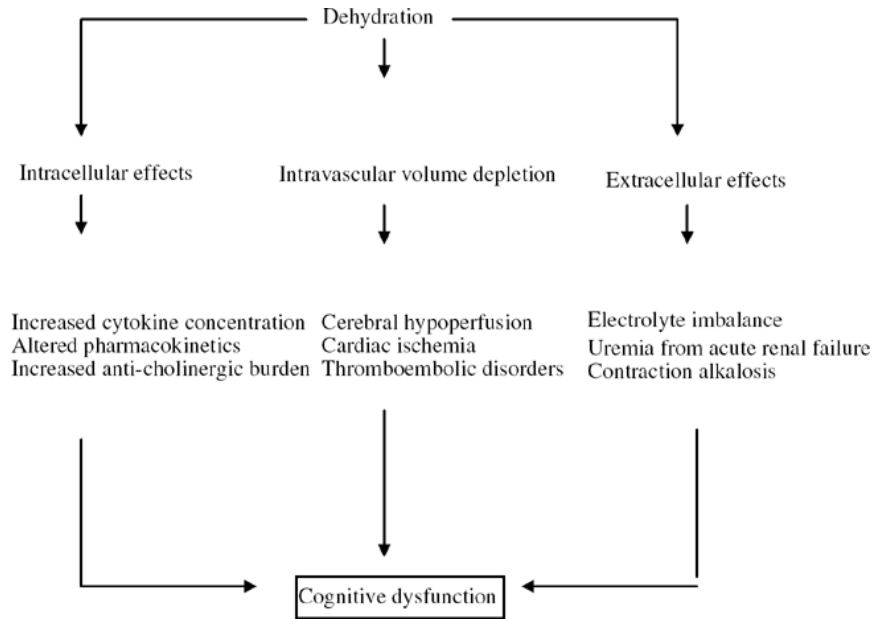


Figure 2. Pathophysiology of cognitive effects from dehydration. Figure from Wilson *et al.*, *European Journal of Clinical Nutrition*, 2003.¹⁵

The physical and cognitive effects of dehydration lead to reductions in performance and severe implications for populations such as soldiers, athletes, and laborers. Physical performance aspects such as strength and endurance have shown to be reduced when in a dehydrated state. Judelson *et al.* found that dehydration significantly reduced the ability of healthy, resistance-trained males to complete a high-intensity resistance exercise challenge, in comparison with hydrated participants¹⁸. Reductions in exercise duration and walking/running distance have been observed in both moderate and hot climates¹⁹. It has been proposed that negative physical performance effects could be due to dehydration-related fatigue caused by the increased cardiovascular strain and thermoregulatory load, and alterations in the ability of the nervous system to stimulate musculature^{18,19}. There is also evidence presented by Armstrong *et al.* that relying on the thirst reflex is not sufficient to avoid dehydration-related decreases in performance in endurance exercise regimens²⁰. Cognitive performance including memory recall, alertness, and subjective cognitive performance, as rated by study participants, have been shown to decrease with increasing dehydration^{21–26}. These reductions in performance and cognition can have a large effect on the manual worker population as this population has been shown to be routinely dehydrated. Coupled with the harsh climates they may be working in; this can be extremely dangerous for this population^{27–30}. For soldiers who are stationed in harsh climates, dehydration can negatively affect their ability to perform routine duties and carry out missions. Finally, for athletes, especially elite athletes where minute differences can have a large impact on the outcome of competitions/races, avoiding dehydration is of the utmost importance.

Methods for Assessing Hydration

Water in the body can be split into two general categories, intracellular water and extracellular water, as shown in **Figure 3**³¹. Intracellular water is the water contained within cells and tissues and constitutes approximately 39% of the body mass. Extracellular water is all of the water outside of cells and includes the water in blood plasma and interstitial fluid; extracellular water makes up approximately 25% of the body mass³². Together, the intracellular and extracellular water makes up the total body water (TBW). Measures of TBW, such as isotope dilution and neutron activation analysis, are considered the gold standard for hydration analysis, although these methods pose numerous limitations that hinder the implementation of the techniques to communities where hydration monitoring is important, such as soldiers, athletes, and manual laborers. Isotope dilution utilizes non-radioactive isotopes of hydrogen or oxygen (e.g. deuterium, deuterium oxide, and oxygen-18) to determine TBW. These isotopes are either orally ingested or administered intravenously and the amount of dilution of the isotope can be measured via sampling body fluid or expired air. The dilution of the isotope directly relates to the amount of TBW⁵. While this technique provides an accurate measure of TBW, it requires 3-5 hours in a laboratory, which makes it not applicable for routine hydration monitoring in the battlefield, sports field, or construction site. Neutron activation analysis can also be used to quantify TBW. This technique requires the use of a nuclear reactor in which the exposure to radiation produces radionucleotides which emit gamma rays during decay. The gamma ray emission can be used to measure the amount of water in the body^{5,33}. This method has numerous disadvantages, such as exposure to radiation, making it inapplicable for routine or repetitive use. A common method for quickly assessing changes in hydration status is by calculating the body mass lost throughout an exercise or study duration. This method relies on the principle that the density of water is 1 g/mL so water lost can be directly calculated from body mass. This method is commonly used in exercise science studies and is often used as a metric when comparing hydration monitoring methods or in the development of a new method for hydration quantification^{34,35}. Despite the widespread use of this technique, it can result in large errors in the estimation of hydration status due to failing to account for respiratory water losses, water generated during substrate oxidation, and mass gained during fat oxidation³⁶. Literature also shows that body mass can fluctuate approximately 0.51 ± 0.21 kg (mean \pm SD) from one day to the next, thus increasing the variability between repetitive experiments and within a study⁵.

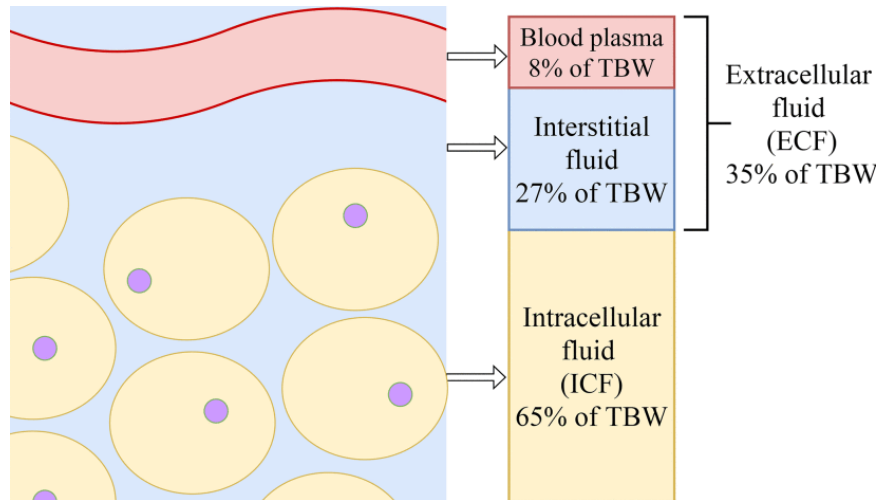


Figure 3. Distribution of total body water (TBW) in the body. Figure from Garrett *et al.*, *IEEE Rev Biomed Eng.* 2017.³¹

Blood analysis is an invasive method that is routinely used for hydration analysis. Plasma osmolality is considered a good metric to describe hydration and represents the concentration of solutes in plasma measured in milliosmoles per kilogram of water (mOsm/kg). Plasma sodium concentration or blood serum osmolality are also regularly used blood metrics for hydration status^{5,37}. While blood metrics have shown good sensitivity for measuring hydration status, they are invasive, time-consuming, and require a phlebotomist, which hinders the implementation of these techniques for use in the battlefield or sports field²². Conversely, collecting urine is non-invasive and does not require specialized personnel for collection so numerous publications cite urine as an advantageous biofluid for hydration assessment. Urine can be analyzed for the osmolality, specific gravity, or color to determine hydration status. The most common method, urine specific gravity, calculates the density of urine in comparison with the density of water to provide a metric of urine concentration²². Urine specific gravity can be measured quickly using a handheld refractometer or disposable test strip. Although test strips have been reported as unreliable, their ease for testing increases the implementation potential of this technique for environments outside of the laboratory^{5,38}. While urine specific gravity is generally considered to be a good metric for assessing hydration, it does have various limitations^{22,39,40}. Previous literature has shed doubt on the use of single urine samples for accurately measuring hydration status⁴¹. Secondly, urinary values have been shown to lag behind blood metrics, since the urine sample contains all the urine collected since the last bladder void^{22,32}. Despite these limitations, urine specific gravity and urine color have been recommended by the National

Athletic Trainers' Association (NATA) and the National Collegiate Athletic Association (NCAA) to safeguard against dangerous levels of dehydration in sport settings^{5,40}.

Other body fluids have been of recent interest as potential indicators of hydration status, including saliva, sweat, and tears. Saliva osmolality can be measured in the same manner as plasma, serum, and urine osmolality. Saliva can be easily collected using salivette swabs or through spitting into collection tubes and is an advantage of utilizing saliva metrics for repetitive hydration assessment. Salivary osmolality has shown an increase in relation to increasing dehydration in numerous studies, but the response was quite variable, indicating a potential drawback of using this method^{37,42-46}. Sweat can be collected using an absorbent collection patch. Dehydration can cause measurable increases in sweat sodium and chloride concentration but currently, studies show variable results^{37,47}. Finally, tear fluid can be collected by having a study participant blink and squeeze their eyes shut. Resulting tear fluid can be collected using a collection vial placed near the eye. Tear fluid osmolality has been shown to increase with increasing dehydration in a few studies, but little research has been conducted analyzing tear fluid for hydration monitoring^{37,48,49}. Another method that has gained attention for measuring hydration is bioelectric impedance. Bioelectric impedance is measured by sending current through tissues to a detector. Both low frequency and high frequencies (5-500 kHz) are used, which allows measurement of intracellular and extracellular water. When compared with TBW values obtained using isotope dilution, bioelectric impedance shows standard error ranging from 1.5-2.9 L, and shows varied success depending on skin temperature and other biological factors⁵⁰⁻⁵⁴.

Given the various limitations of current hydration monitoring techniques, there has been substantial research into novel techniques, including optical, chemical, electromagnetic, and acoustic techniques. Ozana *et al.* developed a speckle-based wrist monitor for glucose and hydration monitoring. While this device is portable, it is unclear the effect that motion would have on the device, thus limiting the implementation potential for this technique⁵⁵. A radio wave absorption device has been developed by Moran *et al.* to measure hydration of tissues and showed high correlation between the developed technique and body weight lost by modeling. This method was only tested on a small population of young males (n=12, 24 ±1 years of age), so there is doubt about the validity of the technique for females and other age populations⁵⁶. A novel microfluidic device developed by Reeder *et al.* has shown the capability of measuring sweat output and alerting the user using a solution of menthol and capsaicin when a high level of sweat has accumulated in the device. Despite the potential benefit of this device, including its wearable nature, sweat rate can vary based on factors other than dehydration, such as fitness level and climate acclimation^{31,57}. Lastly, a handheld acoustic hydration monitor has been developed by Sarvazyan *et al.* This technique measures the speed of sound waves when sent through tissue and correlates it with hydration

status but is confounded by the increase in propagation speed resulting from the elevation of body temperature⁵⁸.

Raman Spectroscopy

Raman spectroscopy (RS) is a vibrational spectroscopy technique that has gained popularity for biological sample analysis due to its non-invasive and non-destructive nature, rapidness, and simplicity. RS is an inelastic scattering technique that provides biochemical information about a sample. When photons interact with a molecule, it can be scattered, either elastically or inelastically. When a photon is elastically scattered, the photon does not experience a change in energy but does experience a change in propagation direction⁵⁹. When a photon is inelastically scattered, or undergoes Raman scattering, the photon may gain or lose energy after interacting with a molecule as well as change propagation direction. In the case of a gain of energy, this is called Anti-Stokes Raman scattering. When the photon loses energy, it is classified as Stokes Raman scattering (**Figure 4**). This change in energy, also called the Raman shift, is the result of the photon perturbing the vibrational or rotational energy levels of the molecule it is incident on⁶⁰. After the scattering event, the photon can travel back to a detector where the change in energy can be measured. The change in energy can be related back to chemical bonds such as C-C stretching, CH₂ scissoring, and C=O vibrations. The location and intensity of the Raman shift can be used to build a biochemical profile of a sample and determine the components present in that sample. The basic instrumentation necessary for collecting Raman spectra includes a monochromatic laser, spectrograph or spectrometer, and detector, such as a silicon CCD or InGaAs camera⁶¹.

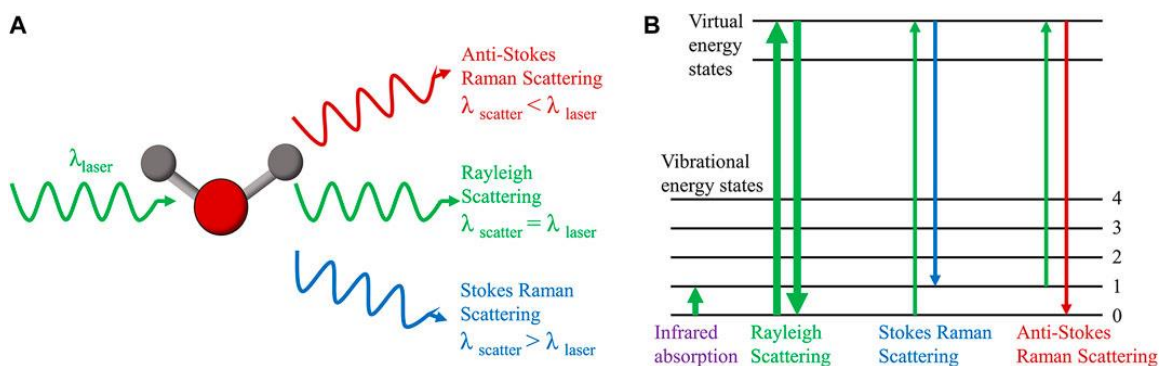


Figure 4. (A) Schematic of anti-Stokes, Stokes Raman scattering, and elastic scattering (Rayleigh scattering); (B) Jablonski diagram of scattering processes showing changes in energy levels. Figure from Liu *et al.*, *Front Bioeng Biotechnol*, 2022.⁶⁰

There are two regions of the Raman spectrum, the fingerprint (FP) region and high wavenumber (HW) region. The FP region ranges from 500-1800 cm⁻¹ and is sensitive to proteins, lipids, blood, nucleic

acids, and various other biochemical components. While this region is the most commonly used for biological sample analysis due to the rich information it gives, it is not advantageous for detecting water content. The main water feature in the FP region resides at 1638 cm^{-1} , which is also the approximate location of a broad amide I peak that is indicative of proteins⁶². The FP water peak is typically low intensity and the amide I peak often overpowers the signal from water at this location, making it difficult to determine water information from the FP region^{63,64}. Conversely, the HW region features a broad water band, from approximately $3000\text{-}3800\text{ cm}^{-1}$. **Figure 5** shows the location and intensity of water features in the FP (left side of the spectrum) and HW region (right side of the spectrum). The HW region not only features a large water feature, but this band also denotes the various hydrogen bonding states that water can participate in. Fully hydrogen bound water is centered at 3075 and 3245 cm^{-1} , partially-hydrogen bound water is centered at 3420 and 3550 cm^{-1} , and free water/unbound water is centered at 3650 cm^{-1} . This information can be used to determine how water is interacting with the environment around it, such as determining the interactions between collagen and water⁶⁵. This richness of information in the HW region makes it the optimal region of analysis for quantifying systemic hydration.

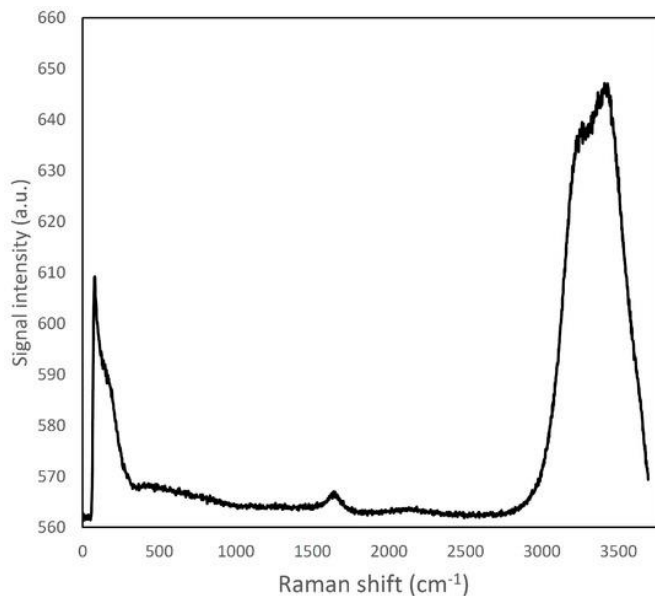


Figure 5. Raman spectrum of pure water showing location and intensity of the FP and HW water features. Figure from Alinovi *et al. Foods*, 2020.⁶

Previous Water Analysis with Raman Spectroscopy

RS has previously been explored for determining localized water content in tissues. In a study by Wolthuis *et al.*, this technique has shown feasibility for assessing water content in localized brain edema. This work utilized a partial least squares regression model to determine water content ranging between 75-

95% in brain tissue, and showed low root mean square error (RMSE)⁶⁶. RS has also been developed for the application of locating tumor margins during tumor resection surgeries. Tumors show an increase in water content, potentially caused by diffusion barriers or leaky vasculature⁶⁷. This prevalence of water in tumor tissues can be exploited via RS to determine the margins of tumors. Previous work in oral squamous cell carcinoma by Barroso *et al.* utilized RS to distinguish cancerous tissue from both tongue tissue and surrounding bone tissue. For distinguishing bone from tumors, a linear discriminate analysis model based on the Raman spectra showed a sensitivity of 0.99 and specificity of 0.83⁶⁸. When analyzing between cancer and tongue tissue, the sensitivity was 0.99 and specificity was 0.92 when analyzing based on the water to protein content ratio⁶⁹. Unal *et al.* used a combination of ratios between the fully and partially hydrogen bound water peaks and the protein peak in the HW region to calculate the amount of mineral-bound water and collagen-bound water. They then further correlated these values with the mechanical properties of bone such as the elastic modulus and toughness⁷⁰. RS has been used to semi-quantify the concentrations of natural moisturizing factors in skin in relation to the hydration of the skin. This work additionally quantified water content between 0-200 μm depth in the stratum corneum⁷¹. Finally, previous work in our group has shown correlation between the water content of the cervix in mice that are pregnant and non-gravid. Spectra were collected from the cervix of non-gravid mice and mice at day 19 of their pregnancy; full-term gestation is reported to be 19.5 days in this mouse colony. Significant changes in the ratio of fully hydrogen bound water to partially hydrogen bound water were observed when comparing the day 19 cervix to the non-gravid cervix, indicating a change in the water dynamics in the pregnant cervix⁶⁵.

Thesis Hypothesis

Based on previous evidence showing the strong potential of RS for measuring localized water content, we hypothesized that RS could be used to determine systemic hydration. Using *in vivo* fiber-optic probe-based RS, we can obtain Raman spectra from individuals in various states of dehydration and correlate spectral features with clinical standards for hydration. This thesis aims to determine the relationship between changes in the Raman spectrum and systemic hydration and to assess the sources of variability in these measurements. Raman features will be compared with clinical standards for assessing hydration to determine the performance of RS in hydration monitoring. The use of RS will enable non-invasive and rapid monitoring of systemic hydration, with the goal of implementing this technique for hydration monitoring in military personnel.

CHAPTER 2: RAMAN SPECTROSCOPY FOR NON-INVASIVE HYDRATION MONITORING: FEASIBILITY AND EVALUATION OF VARIABILITY

Abstract

Dehydration has serious negative side effects including decreasing the body's ability to thermoregulate, inducing cardiovascular strain, and can lead to confusion and delirium. Despite these negative effects, there are currently no non-invasive rapid tools to monitor systemic hydration. Raman spectroscopy is an optical modality with the potential to fill this gap because it is sensitive to water, provides results quickly, and can be applied non-invasively. In this work, high wavenumber Raman spectroscopy was developed toward the detection of systemic hydration via validation with tissue-mimicking phantoms, followed by three *in vivo* studies to investigate the relationship between spectral features and systemic hydration. The Raman spectroscopy-derived metrics used to describe systemic hydration are the area under the curve (AUC) of the water band and the ratio of water features to CH features. A trend in decreasing water band AUC after exercise was identified, although the magnitude of the change was highly variable. In investigating the sources of variability, we identified significant inter-subject variability ($p < 0.05$), and a failure to benchmark our developed technique against clinical standards. Despite the high variability, we found that multiple anatomical locations were suitable for collecting the spectral measurements. While the high degree of variability may confound the use of Raman spectroscopy for non-invasive hydration monitoring, when implementing additional study standardization, significant differences ($p < 0.05$) in spectral metrics can be identified before and after exercise. Raman spectroscopy can potentially allow for rapid, non-invasive detection of systemic hydration, which would improve routine hydration monitoring and reduce the incidence of negative side effects associated with dehydration.

Introduction

The lack of tools to rapidly and non-invasively assess hydration status can be detrimental to military personnel, elite athletes, and other high-performance populations. Dehydration has severe physical and cognitive effects, including increased thermoregulatory stress and cardiovascular strain, and impaired memory and reaction time⁹. Various physiological systems including the gastrointestinal, urinary, and the integumentary system have been shown to be negatively affected by dehydration^{10,11,13,14,72}. Cognition, including memory, alertness, and perception, has been shown to decline with increasing dehydration across numerous age groups⁷³⁻⁷⁷. Dehydration also leads to a decrease in physical and cognitive function, including strength, endurance, and hand-eye coordination^{9,18,21,78,79}. The thirst reflex, or the sensation of being thirsty in response to dehydration, is inadequate to maintain proper hydration in many situations, including long

durations of exercise, exercising in extreme heat, high intensity exercise, and in the elderly population. Thus, in these scenarios, without routine hydration monitoring, significant dehydration may occur leading to the negative effects previously detailed⁸⁰.

Despite its importance, there are currently no widely accepted gold standards for quantifying hydration. While quantifying total body water is sometimes considered the gold standard, this analysis is impractical for routine or repetitive use³². More commonly used methods are not rapid and non-invasive, such as blood, salivary, or urine metrics. Plasma osmolality measures the solutes present in plasma, and relies on sample collection by trained personnel, analysis in a laboratory, and may only be sensitive to severe fluid loss⁸¹. Urinary measures reflect all the urine that has accumulated in the bladder since the last bladder void, rather than providing real-time hydration information²². Saliva markers have shown high variability and are easily confounded when fluid and food intake is not restricted⁴⁵. Finally, body mass change over an exercise period is one of the easiest and most used methods, yet poses issues such as failing to account for respiratory water loss and weight lost from the metabolism of carbohydrates, fat, and protein, which can introduce significant errors into the calculation³⁶. Emerging techniques to measure hydration status include optical monitoring and electrochemical sensors^{31,43,44,82-86}. While all these techniques show significant limitations, Raman spectroscopy is advantageous for this application due to its non-invasive nature, ability to provide results quickly, and simplicity.

Raman spectroscopy (RS) is a sensitive and non-invasive optical modality that shows potential for real-time hydration monitoring. RS is an inelastic scattering technique that provides information related to the biochemical components of a sample⁸⁷. The location and intensity of Raman features can be used to determine the chemical structure of molecules, identify chemicals and biomolecules present in a sample, and analyze solutes quantitatively^{88,89}. RS is advantageous over other techniques due to its sensitivity and measurement speed⁹⁰. The Raman spectrum is made up of two regions, the fingerprint region (FP) from 500-1800 cm^{-1} and the high wavenumber region (HW) from 2800-3800 cm^{-1} ⁶⁵. The FP region shows limited water information, as the water features in the FP region are in the same location as strong protein and lipid features ($\sim 1640 \text{ cm}^{-1}$)⁶³. To overcome this limitation, we are using HW RS, which shows rich water information relating to OH stretching between 3000-3800 cm^{-1} ^{62,65}. This region allows analysis of water content and the dynamics of water hydrogen bonding, as previously reported in literature^{65,91,92}.

Previous use of RS for water content analysis has focused on localized determination of water content including assessing brain edema, analyzing tumors, determining bone mineral ratios, and identifying natural moisturizing factors in skin. RS has been demonstrated to accurately predict the percentage of water in brain tissue by utilizing partial least-squares regression⁶⁶. The use of RS for intraoperative assessment of tumor margins has been proposed, as cancerous tissue has been shown to

contain a higher percentage of water than normal tissue⁶⁷. This technique has shown efficacy for discriminating oral squamous cell carcinoma from healthy tongue and bone tissues and breast cancer from surrounding tissues^{68,69,93-95}. RS has also been applied to study the percentage of collagen and mineral-bound water in bone and its relationship to the mechanical properties of bone⁷⁰. Finally, RS has also been used to determine the concentration of water and natural moisturizing factors in the skin⁷¹. Our group has previously demonstrated that RS can detect differing water content in the cervix of pregnant mice. *In vivo* RS was used to compare the hydration of the cervix in pregnant and nonpregnant mice and was able to detect significantly different water content between the two groups⁶⁵. While RS has been used to investigate water content previously, this is the first demonstration of the technique for quantifying systemic hydration, to the best of our knowledge.

This study aimed to investigate the feasibility of HW RS to monitor changes in systemic hydration and evaluate sources of variability toward the implementation of RS for hydration monitoring. Toward this goal, *in vivo* RS was used to determine the hydration of exercising individuals and spectral features were analyzed to determine changes associated with changing levels of hydration. Additionally, various sources of variability were assessed including inter-subject variability, variability between clinical standards, and between repetitive measurements. Utilization of RS for hydration monitoring offers a rapid, non-invasive method for measuring hydration which can be beneficial in identifying potentially dangerous dehydration.

Methods

Raman spectroscopy system

For this study, Raman spectra were acquired on two fiber-optic probe-based Raman systems. System 1 consists of a diode laser (680 nm) (1804B000 Fat Boy, Innovative Photonic Solutions) coupled to a custom-designed fiber-optic probe (EmVision, LLC) containing one excitation fiber (300 μm , 0.22 NA) and 17 collection fibers (300 μm , 0.22 NA) organized in three concentric circles around the excitation fiber (3 fibers in inner ring, 5 in middle ring, and 9 fibers in the outer ring) (**Figure 6A**). The collection fibers deliver the backscattered light to an imaging spectrograph (HT spectrograph, EmVision, LLC) which disperses the light onto a thermoelectrically cooled, deep depleted CCD camera (Pixis 400BR, Teledyne Princeton Instruments). The system has a spectral resolution of 8 cm^{-1} . System 2 utilizes the same 680 nm wavelength laser diode coupled to a fiber-optic probe with one excitation fiber (200 μm , 0.22 NA) with 30 collection fibers (300 μm , 0.22 NA) (EmVision, LLC) organized in three concentric circles (6 fibers in inner ring, 9 fibers in middle ring, and 15 fibers in the outer ring) (**Figure 6B**). The fiber optic probe is coupled to an imaging spectrograph (LS785, Teledyne Princeton Instruments) which disperses the light onto the same thermoelectrically cooled, deep depleted CCD camera as used in System 1. The spectral

resolution of System 2 is 5 cm⁻¹. Both systems are controlled with a laptop and custom LabVIEW program. For both systems, only the data collected from the inner ring of fibers was analyzed in this study.

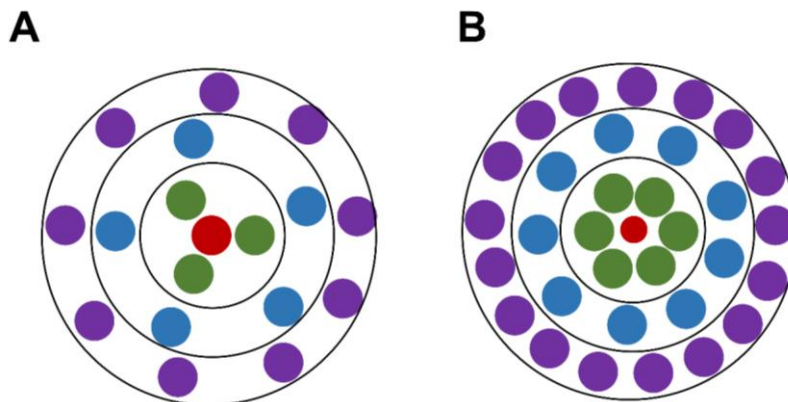


Figure 6. Diagram of fiber optic probe layout for System 1 (A) and System 2 (B). The red fiber represents the excitation fiber. The green fibers represent the inner fibers; blue fibers represent the middle fibers, and the purple fibers represent the outer fibers.

Tissue-mimicking phantom validation

Tissue-mimicking gelatin phantoms were created with water content ranging from 65-90% water in 5% increments, which is representative of the water content found in most human tissues⁶⁵. To prepare gelatin phantoms, gelatin powder was slowly added to deionized water and mixed over gentle heating. Once all the gelatin was dissolved, the mixture was poured into molds and allowed to cool to room temperature. Each phantom was then removed from the molds and placed on top of aluminum foil for RS measurements. System 2 was used for spectra collection from tissue mimicking gelatin phantoms. The fiber-optic RS probe was placed in light contact with each phantom and spectra were acquired for five seconds using 50 mW of laser power at 680 nm. Five measurements were taken per phantom to account for heterogeneity in sample preparation and they were averaged.

***In vivo* studies**

To assess spectral changes associated with varying levels of dehydration, three phases of *in vivo* studies were performed. All study participants were enrolled using informed written consent under a protocol approved by Vanderbilt University's Institutional Review Board following the guidelines of the Declaration of Helsinki. In total, 34 participants took part in this study with n=10 in study 1, n=19 in study 2, and n=5 in study 3. Participant demographics for each study are shown in **Table 1**.

Table 1. Participant demographics for *in vivo* studies.

Participant Demographics	
Study 1	
n:	10
Age:	26.4 ± 5 years
Gender:	5M, 5F
Study 2	
n:	19
Age:	26.5 ± 10.2 years
Gender:	10M, 9F
BMI:	22.9 ± 2.6 kg/m ²
Study 3	
n:	5
Age:	25.8 ± 1.9 years
Gender:	3M, 2F
BMI:	24.1 ± 3.3 kg/m ²

In vivo protocols

Three exercise protocols were utilized for the *in vivo* studies and ranged from non-standardized exercise to standardized intensive exercise (**Table 2**). In Study 1, participants were asked to exercise between 25-45 minutes and could choose the type of exercise they performed. The exercises performed included running, power walking, and cycling. In Study 2, participants completed a standardized workout consisting of a 20-minute session on an indoor rowing machine (resistance level 5) followed by a 20-minute high intensity interval training (HIIT) workout. For Study 3, only participants who routinely exercised (e.g., exercised 3 or more days per week) were enrolled. Participants were asked to complete a 10 km self-paced run within one hour. Additionally, for Study 3, each participant engaged in a pre-exercise hydration protocol that consisted of drinking 500 mL of water the night before the study and 500 mL the morning before arriving to the laboratory to ensure all participants were below the euhydrated urine specific gravity threshold of 1.01⁹⁶. For all three studies, participants' water intake was minimal, and it was recorded.

Table 2. Overview of exercise protocols utilized in each *in vivo* study.

In Vivo Study Protocols			
	Study 1	Study 2	Study 3
	Non-standardized exercise	Standardized moderate exercise	Standardized intense exercise
	n = 10	n = 19	n = 5
Exercise Performed	Running, power walking, cycling, etc.	20-minute row on indoor rowing machine at resistance level 5 & 20-minute high-intensity interval training session	10 km run
Exercise Duration	25-45 minutes	40 minutes	1 hour or less
Clinical Standards Collected	N/A	Urine specific gravity, weight lost during exercise	Urine specific gravity, weight lost during exercise
Enrollment Criteria	N/A	N/A	Exercised 3+ days per week, comfortably run 10 km in under 1 hour

Raman spectra collection

For all three studies, Raman measurements were collected before and after the exercise period. System 2 was utilized for Study 1 and 2 and System 1 was utilized Study 3. 50 mW of laser power (680 nm) was used for spectral collection in this study and was calibrated prior to each study participant. The Raman probe was held by each participant and placed in light contact with the skin for the measurement collection. In Study 1 and 2, measurements were taken from four locations on the body to determine if there is an optimal location for collecting spectral information related to hydration. The locations measured were the top of the hand (dorsal hand), the inside of the wrist, the inner bicep, and the back of the knee, and were chosen to investigate the influence of skin thickness, sweat rate, and upper vs lower body. For Study 3, measurements were collected from the inside of the wrist and inner bicep. Each location was wiped with an alcohol wipe prior to collecting the spectral measurement to reduce spectral contributions from contaminants on the skin. For study 1 and 2, 20 second accumulations were collected and for study three, 10 second accumulations were collected. For all 3 studies, each participant held the fiber optic probe themselves. In Study 3, measurements at each location were repeated three times to assess measurement homogeneity. To collect these repetitive measurements, each participant removed the probe from the measurement area and replaced it in approximately the same location.

Clinical standard collection

For Studies 2 and 3, two clinical standards were used to assess hydration: urine specific gravity (uSG) and body weight lost during exercise (**Table 2**). Participants were given a sterile specimen collection cup and they provided a urine sample before and after the exercise period. Each urine sample was stored at room temperature until analysis that was performed within 12 hours of collection. To determine the uSG, each sample was gently mixed by pipetting up and down four times and 300 μ L of the sample was pipetted onto the prism of a handheld urine refractometer (PAL-10S Pocket Urine Refractometer, ATAGO) (**Figure 7**). The sample temperature was allowed to stabilize for 15 seconds on the prism prior to recording the uSG value. Each sample was measured three times to ensure reproducibility. Between each sample measurement, the refractometer was cleaned with 70% ethanol and deionized water. To calculate body weight change after exercise, each participant was weighed on a digital scale (Ozeri ProMax, Ozeri) before and after the exercise period.



Figure 7. ATAGO digital handheld refractometer used for uSG measurements. Figure adapted from ATAGO.com.

Data processing and analysis

The same data processing and analysis protocol was used for data collected on both Raman systems. Spectra were collected by capturing the full image of the CCD output. A curvature correction was applied to each image, due to the spectrograph optics inducing a curvature in the fibers. Subsequently, each image was segmented into 3 regions of interest, representing the concentric collection fiber organization in the fiber-optic probe. For all analysis, only the inner most fiber region was used. Spectra were calibrated using the spectral peaks of a neon argon lamp, 4-acetamidophenol, and cyclohexane, following established

processing methods^{65,97–102}. Intensity calibration was performed using a NIST calibrated tungsten lamp and daily calibration was performed using a piece of green glass. Spectra were smoothed with a 3rd order Savitzky-Golay filter with a frame length of 7¹⁰³. Lastly, the fluorescent background was subtracted by fitting with a 3rd order polynomial function (**Figure 8**). Two analysis metrics were chosen: the area under the curve (AUC) of the water band, and the ratio of water features to CH features. The AUC of the water band was calculated by integrating between 3050–3600 cm^{-1} . To calculate the ratio of water features to CH features, the AUC of the water band (3050–3600 cm^{-1}) was divided by the AUC of the CH band (2850–2965 cm^{-1})^{62,65,71}. To determine the degree of change between pre-exercise and post-exercise spectral metrics, the percent change was calculated by subtracting the pre-exercise metrics from the post-exercise metrics and dividing by the pre-exercise metric. All spectral processing and analysis were performed in MATLAB 2021 (Mathworks).

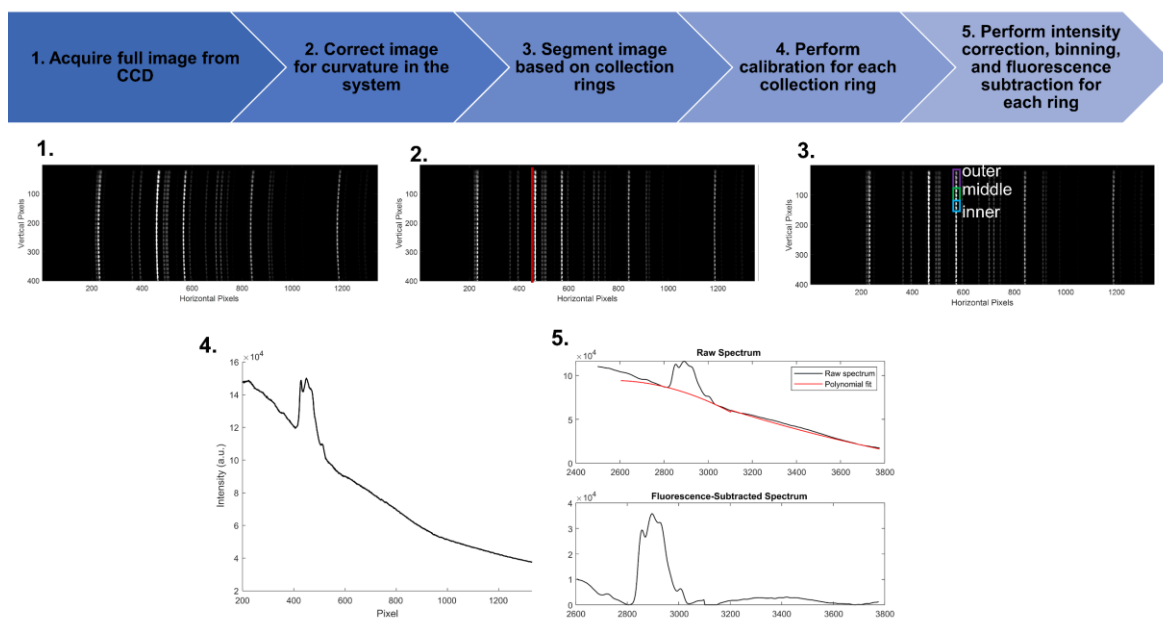


Figure 8. Flowchart of Raman data processing protocols.

Statistical analysis

The water band AUC and water to CH ratio of the gelatin phantoms were analyzed using a one-way ANOVA. Two-way ANOVAs were used to determine the significance of inter-subject variability. The variance between the different locations was analyzed using a Brown-Forsythe test for equal variance. To determine the correlation between the AUC of the water band, the uSG percent change, and weight loss percent change, Pearson correlation tests were performed. Pearson correlation was also used to determine

the relationship between uSG percent change and weight loss percent change. An F-test was performed to determine significant differences between the female and male groups clinical standards and AUC of the water band distribution. A two-way ANOVA was used to determine the sources of variability within Study 3, and t-tests were used to determine the significance of the difference between the pre-exercise and post-exercise water band AUC of each participant. An alpha value of 0.05 was used for all statistical analyses. Statistical analysis was performed using GraphPad Prism 9 (GraphPad Software). All data are presented as mean \pm standard deviation, except where otherwise indicated.

Results

Gelatin-based phantoms

Gelatin-based tissue-mimicking phantoms at various hydration levels were measured to determine the optimal spectral metrics for assessing hydration status. With an increase in known water content, from 65% to 90% water in 5% increments, there is an observable increase in the amplitude of the water band (**Figure 9A**). From this data set, two spectral metrics were identified: AUC of the water band and the ratio of water features to CH features. The percentage of water in the gelatin phantoms was plotted against the water band AUC (**Figure 9B**). This shows that there is a statistically significant increase in the AUC of the water band as the water content in the gelatin phantoms increases ($p < 0.0001$). Additionally, the ratio of water to CH features was plotted against the known phantom water content, and a statistically significant increase in the ratio in response to increasing water content is shown ($p < 0.0001$) (**Figure 9C**).

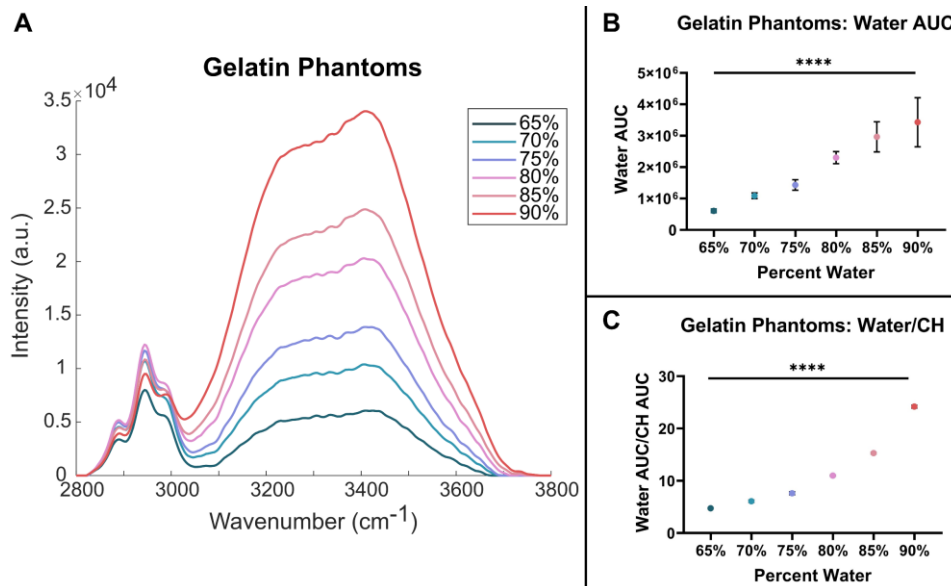


Figure 9. Gelatin-based phantoms with varying water content. (A) HW RS spectra of gelatin phantoms with water content from 65-90%; (B) the water band AUC (mean \pm SD) for each water concentration showing significant increase in AUC as water content increases; (C) water to CH ratio (mean \pm SD) showing significant increase in ratio as water content increases (**** $p < 0.0001$).

The relationship between spectral metrics and changing hydration was evaluated by calculating the percent change from before to after exercise. **Figure 10** shows the water band AUC metric plotted based on the location the spectra were collected for Study 2 (**Table 2**). It can be observed that the majority of the percent change values are negative, indicating a decrease in the AUC of the water band after exercise, which represents a decrease in the participant's hydration following the exercise regimen. While most of the percent change values are negative, the magnitude of the change varies greatly, between -47% to -0.67 % in the wrist location, for example. Additionally, for each location there are at least 3 or more data points that are positive percent changes, indicating there was an increase in water band AUC after exercise. The high degree of variability in magnitude and direction of the percent change values led us to assess the sources of variability present.

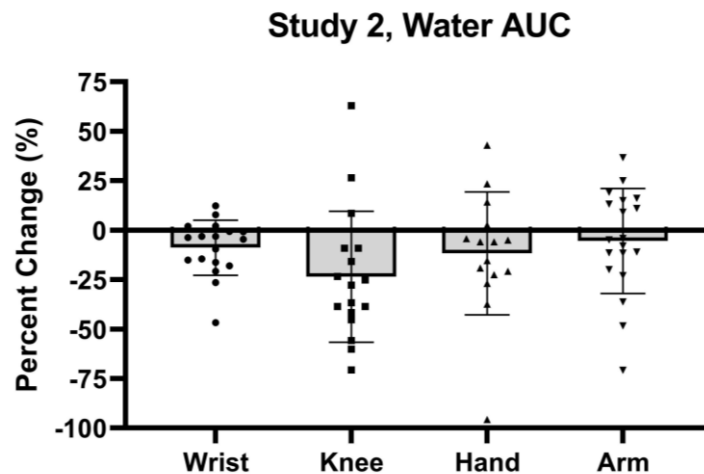


Figure 10. Water band AUC percent change for each location in Study 2. Percent change of the AUC of the water band for each location demonstrating a general trend of negative percent change values, indicating a trend in decreasing water band AUC after exercise, but high degrees of variability in magnitude are seen.

Inter-subject variability

One of the largest sources of variability throughout our studies was inter-subject variability. For Study 2, inter-subject variability was significant ($p < 0.05$) and accounted for over 69% of the variability at each location (**Figure 11**). This variability between subjects highlights one of the largest difficulties in developing this non-invasive RS-based hydration monitoring technique. The degree of inter-subject variability identified here could make it difficult to identify changing hydration due to the variability overshadowing the minute changes we are trying to identify.

Source	Percent of total	P value	Significant?
Arm			
Time (Pre vs Post)	1.4%	0.2048	No
Subject	83.9%	0.0003	Yes
Wrist			
Time (Pre vs Post)	3.6%	0.0138	Yes
Subject	88.3%	<0.0001	Yes
Knee			
Time (Pre vs Post)	7.4%	0.0178	Yes
Subject	74.5%	0.0029	Yes
Hand			
Time (Pre vs Post)	5.7%	0.0944	No
Subject	69.4%	0.0325	Yes

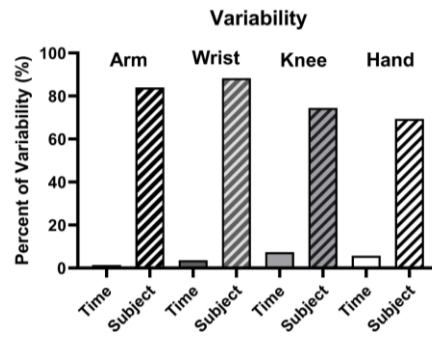
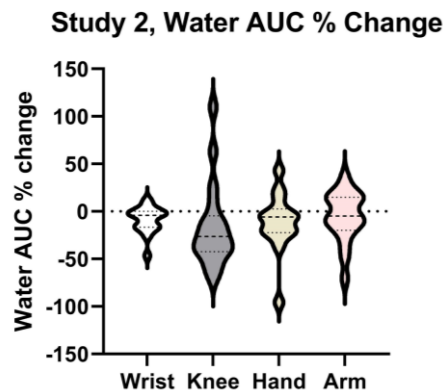


Figure 11. Analysis of inter-subject variability. (A) Analysis of variance (ANOVA) results for each location highlighting large amount of inter-subject variability; (B) graphical representation of sources of variability.

Optimal location

To determine if there is an optimal location for collecting RS-based hydration measurements, spectra were collected from four locations: the top of the hand (dorsal hand), the inside of the wrist, the inner bicep, and the back of the knee. For each location, the percent change in the AUC of the water band was plotted from Study 2, and the standard deviation (SD) and range of percent change values was calculated (**Figure 12**). A test of equal variance was performed to determine if one location showed less variability than others, but the results reveal that no location was less variable than the others tested ($p=0.76$). Despite the non-significance, the wrist location showed the lowest range and SD, so this location was chosen for the rest of the analysis.



	Wrist	Knee	Hand	Arm
Range	59.08	180.4	138.6	107.3
SD	13.94	44.94	31.04	26.56

Figure 12. Analysis of four measurement locations. Violin plot of the percent change of the AUC of the water band for the four locations measured and the range and standard deviation (SD) of the percent change values for the four locations.

Exercise standardization

The effect of standardizing the exercise type and duration was investigated by comparing the AUC of the water band and water to CH ratio across the three *in vivo* studies. Study 1, which utilized unstandardized exercise type and duration, showed the largest range and SD in percent changes values for both metrics (**Figure 13**). Study 2, the moderate standardized exercise protocol, showed smaller ranges and SD for both metrics. This trend of decreasing range and SD continued in Study 3, which consisted of an intense standardized exercise regimen, for the water to CH ratio but was not the case for the AUC of the water band. The AUC of the water band showed a decrease in range but not SD for Study 2 and Study 3.

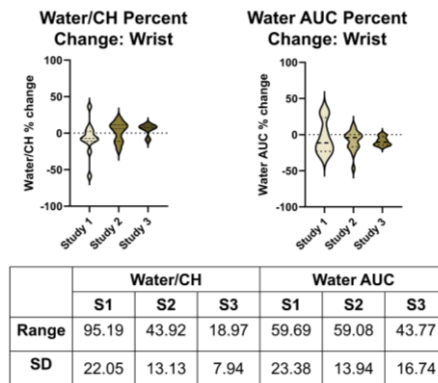


Figure 13. Analysis of effect of exercise intensity and standardization. Violin plots of the percent change of the water to CH ratio (left) and AUC of the water band (right) and the range and SD of percent change values showing the effect of increasing exercise standardization from Study 1, 2, and 3. (S1: unstandardized exercise, S2: standardized moderate exercise, S3: standardized intense exercise).

Hydration standards

An important step toward developing RS for non-invasive hydration monitoring is to benchmark the technique against currently used methods for hydration assessment. The two standards chosen for these studies are urine specific gravity (uSG) and body weight change. The uSG percent change and the percent change in the AUC of the water band were plotted and the Pearson correlation coefficient was calculated between the two values (**Figure 14A**). The correlation coefficient was calculated as $r=0.088$, indicating no correlation between the two metrics. This process was repeated using the body weight change (**Figure 14B**). The correlation coefficient between body weight change and percent change of the water band AUC was calculated to be $r= -0.144$, indicating a weak correlation. When comparing the two standards to each other, the Pearson correlation coefficient was calculated to be $r=-0.11$, indicating weak correlation (**Figure 14C**).The lack of correlation between the two standards may indicate that these commonly used metrics aren't the optimal standards to be used when developing a novel hydration monitoring technique, and other methods should be explored, such as blood indices.

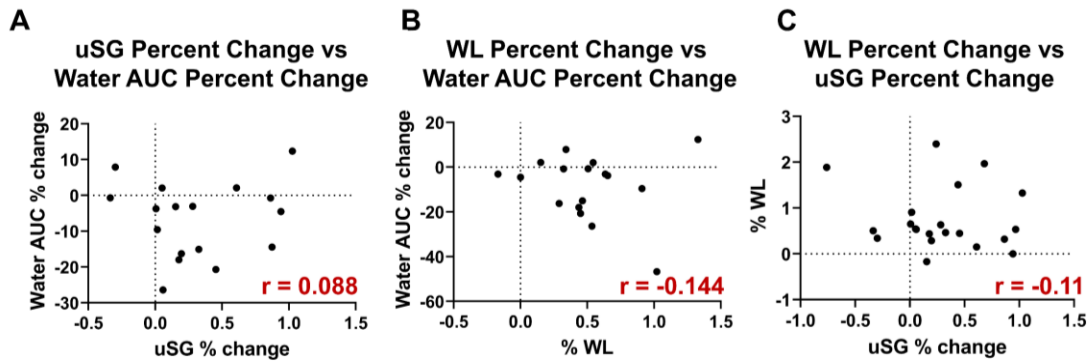


Figure 14. Clinical standard correlation. Scatter plots of the water band AUC and uSG percent change (A) and weight loss percent change (B) with the Pearson correlation coefficient showing weak or no correlation between the metrics. (C) Scatter plot of uSG percent change and weight loss percent change with the corresponding Pearson correlation coefficient showing weak correlation.

Gender variation

To investigate potential causes of the weak correlation between the two commonly used hydration assessment techniques, we separated the data by gender, as literature shows there may be differences in the dehydration dynamics between females and males^{104–108}. We identified no difference between the uSG percent change between the male and female group but saw significant difference between the weight loss percentage between the two groups (**Figure 15A**). The male group's weight loss percentage was clustered more tightly and showed significantly different variance than the female group's percent weight loss ($p=0.0008$). When segmenting the AUC of the water band by gender, a similar pattern of the male group being clustered more tightly than the female group was observed (**Figure 15B**). The variance was nearly significantly different ($p=0.0535$) for the AUC of the water band. Lastly, the Pearson correlation coefficients were recalculated with the data grouped by gender. In all cases, grouping by gender increased the magnitude of the correlation coefficient, but all correlations remained below 0.5, indicating weak ($r<0.3$) or moderate ($0.3<r<0.5$) correlation (**Figure 15C**). The correlation between the two standards were also recalculated when grouped by gender, and the correlation coefficients increased in magnitude (Male: $r=-0.28$, Female: $r=0.17$), but remained only weakly correlated. Analyzing by gender may help to benchmark the developed RS technique against currently used hydration assessment methods but does not substantially affect the agreement between the two standards used in this study.

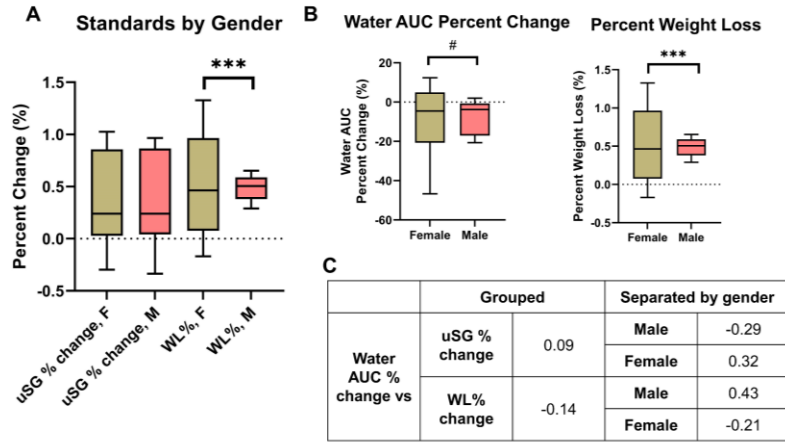


Figure 15. Analysis of gender effects. (A) Clinical standards separated by gender highlighting the significant difference in distribution between the weight loss percentage of males and females; (B) water band AUC grouped by gender displaying a similar distribution as the percent weight loss for each gender; (C) Pearson correlation coefficient calculated for the total group (left side) and when data is separated by gender (right side), showing an increase in magnitude in correlation when grouped by gender. (**p<0.001, #p=0.0535).

Repetitive measurement variability

In Study 3, we controlled for additional factors such as ensuring all participants were not dehydrated before the study and only enrolled participants who were well conditioned for the exercise regimen (**Table 2**). The final change made in Study 3 was to implement repetitive spectral measurements, where three measurements were taken from each location before and after the exercise regimen. These repetitive measurements allowed us to assess the homogeneity between measurements. The repetitive measurements were highly variable for some participants, as highlighted by participant 3 in **Figure 16A**. The repetitive measurements were also found to be a significant source of variability (**Figure 16B**). Despite the high degree of variability seen within the repetitive measurements, there was a trend of decreasing AUC of the water band after exercise as compared to before exercise, with significant decrease observed in two of the four participants (**Figure 16C**). This indicates that despite the high variability between measurements, there is still a large difference between pre- and post-exercise hydration that is detectable using RS. P1 was not included in this analysis due to only one measurement being taken at each location before and after exercise.

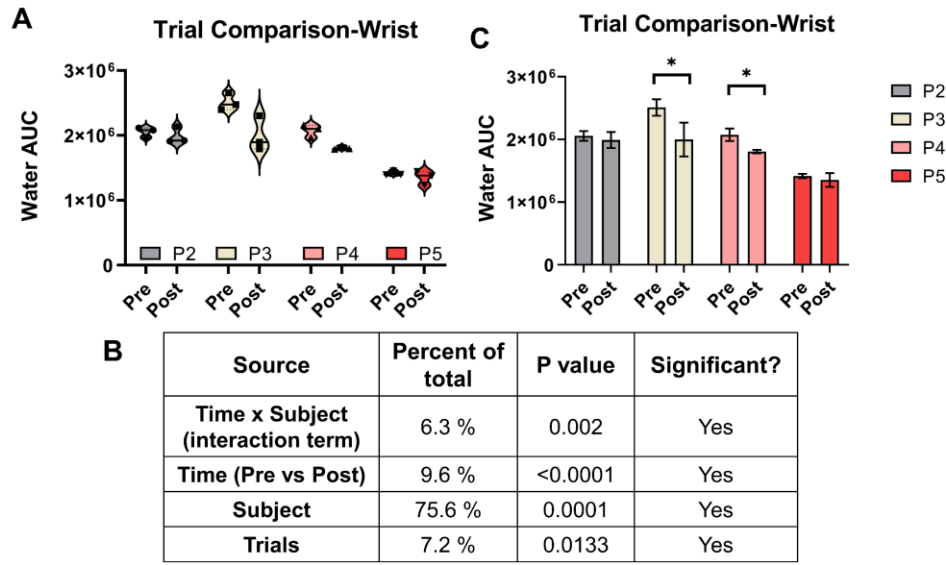


Figure 16. Inter-measurement variability in Study 3. (A) Violin plots of repetitive measurements for P2-P5 showing high degree of variability between repetitive measurements; (B) Analysis of variability (ANOVA) results show significant inter-trial variability (C) Bar plots (mean \pm SD) representing trend in decreasing water AUC after exercise with two participants (P3 and P4) showing a significant decrease after exercise (* p <0.05).

Discussion

In this study, a RS method for non-invasive monitoring of hydration has been developed. This method has been demonstrated to show changes in water content in gelatin tissue-mimicking phantoms correlated with two spectral metrics, the water band AUC and water to CH ratio. Furthermore, preliminary results from *in vivo* studies indicate that spectral features show changes in systemic hydration, though a large degree of variability exists. Factors such as exercise standardization, measurement heterogeneity, and inter-subject variability must be taken into account to develop RS for accurate hydration monitoring. Utilizing RS for hydration monitoring is advantageous because the method is rapid, non-invasive, and simplistic.

Gelatin phantoms of varying water content show a distinct spectral response to the changing water content. It can be observed that there is an overall increase in the intensity of the water band, from 3100-3600 cm^{-1} (**Figure 9A**). This band increased incrementally as the known water content in the gelatin phantom increased, indicating a direct spectral response to the increasing water content. To investigate the optimal quantitative spectral metric for assessing water content and hydration status, we identified two metrics from this gelatin phantom study: the ratio of water features to CH features, and the AUC of the water band. The ratio of water features to CH features, representing protein and lipid contributions, has

previously been shown to correlate well with known water content, thus this metric was used in the present gelatin phantom study^{69,71}. There was a significant increase in the water to CH ratio ($p < 0.0001$), indicating that this metric described water content accurately in the present study (**Figure 9C**). The other metric chosen, the AUC of the water band, was chosen to exclusively look at water features, as there may be varying protein and lipid contributions under the skin when translating this technique *in vivo*^{109,110}. This metric also showed a significant increase ($p < 0.0001$) in water band AUC with an increase in known water content in the gelatin phantoms (**Figure 9B**). This study not only confirmed that RS can detect changes in water content but identified two key spectral metrics for describing water content using RS, which were then utilized in our *in vivo* studies.

After determining the relationship between water content and spectral metrics in gelatin phantoms, we performed three *in vivo* studies to investigate the relationship between spectral metrics and systemic hydration. When analyzing our study with the most participants, Study 2 ($n=19$), the percent change of the AUC of the water band was plotted for each location (**Figure 10**). The majority of percent change values were negative, indicating a decrease in water band AUC after exercise as compared to before. Based on the results from the gelatin phantoms that show that the AUC of the water band increases with increasing hydration, this negative percent change could be attributed to decreasing hydration. The magnitude of percent change does vary greatly; for example, the percent change in the wrist location ranges from -47% to -0.67%.

Furthermore, we hypothesize that the magnitude of percent change of the water band AUC varies largely for a few reasons. Upon further analysis, we found that the starting hydration of our participants varied greatly (**Figure 17**). Between Study 2 and 3, 14 participants were well hydrated ($uSG < 1.01$), and 10 were either minimally ($1.01 < uSG < 1.02$) or moderately dehydrated ($uSG > 1.02$), based on uSG cutoff values reported by the National Athletics Trainers Association⁹⁶. This pre-exercise dehydration could have impacted the intensity at which each participant conducted the study exercise, thereby decreasing their dehydration during the exercise protocol¹¹¹. The exercise regimen was also kept constant, despite differences in gender, body type, and exercise conditioning, which could have affected the performance of some participants, thus reducing their amount of dehydration. While most percent change values were negative, at each measurement location, there were at least three values which were positive, indicating an increase in hydration throughout the exercise. These increases in water band AUC are hypothesized to be due to differences in the placement of the fiber optic RS probe when collecting measurements. Adipose tissue only contains approximately 5-10% water while the skin and muscle contain a much higher proportion of water at 40% and 75%, respectively^{104,112,113}. Due to these large differences in water content based on tissue type, if a measurement is taken in a location that has a larger proportion of subcutaneous

fat or has heterogeneity in subcutaneous fat distribution, the RS metrics may not accurately reflect the systemic hydration status. Despite the few positive percent change values, the majority of values were negative, indicating that RS can detect changes in hydration after exercise.

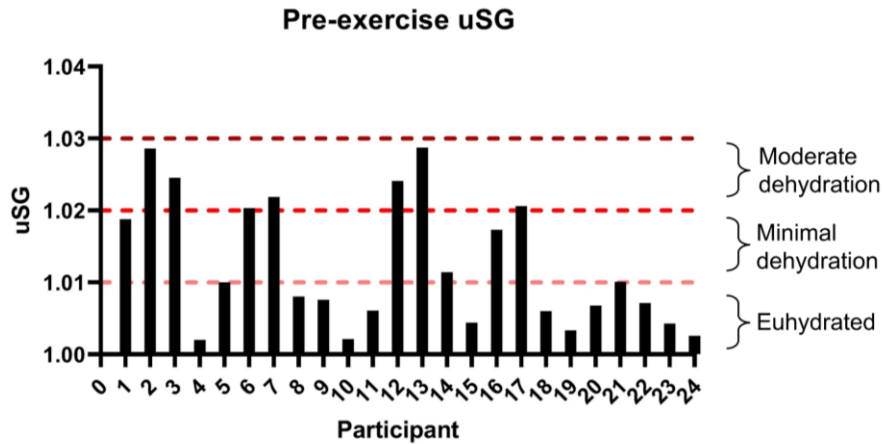


Figure 17. Participant pre-exercise hydration. Pre-exercise urine specific gravity (uSG) values for participants in Study 2 (P1-19) and Study 3 (P20-24) highlighting varying levels for pre-exercise hydration.

To identify sources of variability, two-way ANOVAs were performed using the data collected in Study 2 for each location. This determined that there was a significant contribution of variability between subjects, with inter-subject variability responsible for at least 69% of variability at each location (**Figure 11**). While some degree of inter-subject variability can be expected, the large degree found in this study could present a challenge in the development of an RS tool for assessing hydration. The large amount of variability can overshadow the spectral changes we may see due to changing hydration status. We hypothesize that the overarching inter-subject variability could be caused by a few factors. Differing levels of pre-exercise hydration, as shown by the pre-exercise uSG values in **Figure 17**, could have affected the exercise intensity each participant was able to perform and could have affected the net water loss during the exercise. Additionally, while all participants in Study 2 followed the same exercise protocol, which increased the standardization of the study, this does not allow for personalization of the exercise protocol to each participant’s ability level. In this study, we enrolled participants who exercised 0-1 times per week as well as participants who exercised 4 or more times per week. When subjecting these participants to the same exercise regimen, it is expected that the participants who routinely exercise weekly may be able to perform more highly, thus dehydrate more during the same time period. The lack of exercise personalization may have contributed to the large degree of inter-subject variability and can be addressed in future studies

to decrease this type of variability. By taking these factors into account, we aim to decrease the significance of inter-subject variability in future studies.

In developing a RS-based method for assessing systemic hydration status, it is important to take the measurement location into consideration. Throughout the *in vivo* studies described here, four locations were tested: the top of the hand (dorsal hand), the inside of the wrist, the inner bicep, and the back of the knee. These locations were chosen to determine the influence of local sweat rate, skin thickness, and upper body vs. lower body on the spectral metrics. Literature shows that the regional sweat rate varies greatly, with the dorsal hand, back of the knee, and inner bicep showing low to moderate sweat rate while the wrist shows a high sweat rate^{114,115}. The skin thickness at the locations chosen ranged from lower at the wrist and hand locations and higher at the upper arm and knee locations¹¹⁶. We also wanted to identify if upper body vs. lower body would have an effect on the spectral measurements because increased blood flow heterogeneity during exercise in the upper body, specifically the arms, could affect water diffusion and distribution in the upper body¹¹⁷. When comparing the percent change values of the AUC of the water band from the four locations, we found no statistical difference between the variance of the locations (**Figure 12**). This shows that none of the locations are more variable than the others, and the physiological factors such as regional sweat rate and skin thickness may not have a large impact on the RS measurement. This is important toward the implementation of RS-based hydration monitoring as it shows that the measurement could be taken at various locations on the body. This makes the technique adaptable to the various scenarios and populations it may be implemented in, such as in military or athletic populations.

Throughout the *in vivo* studies we performed, the exercise regimen got progressively more standardized and more rigorous (**Table 2**). This included standardizing both the duration and type of exercise performed. To examine the effect of exercise standardization on the variability in spectral metrics, we plotted the percent change of the water to CH ratio and the percent change of water band AUC for each study (**Figure 13**). As the exercise standardization increases, the range of percent change values decreases for both metrics. Additionally, the standard deviation of the percent change values decreased as the study standardization increased for the water to CH ratio. For the percent change of the water band AUC, the SD decreased from Study 1 to 2 but rose slightly for Study 3. We hypothesize that this is due to the low sample size (n=5), but further data collection is needed to confirm this hypothesis. The results indicate that highly standardized studies are necessary to develop this RS-based method for assessing systemic hydration. Highly standardized studies must be conducted to ensure a satisfactory baseline understanding of how spectral features change in response to varying levels of systemic hydration. Following highly controlled studies, more variable, real-world data collection can take place that is more representative of the use cases, such as at a sports game or in the battlefield.

To benchmark the developed RS-based method for assessing systemic hydration, two commonly used hydration assessment techniques were chosen to be clinical standards. Weight loss percentage is one of the most commonly used metrics in exercise studies and urine specific gravity (uSG) is widely used in medical clinics, by sports associations (e.g. National Collegiate Athletics Association [NCAA]), and in various exercise studies^{5,32,40}. Despite the widespread use of these techniques, we identified low or no correlation between the water band AUC and either metric with a Pearson correlation coefficient of 0.088 for the uSG percent change and -0.144 for the percent weight lost (**Figure 14A-B**). We additionally found minimal correlation between the two standards with a Pearson correlation coefficient of -0.11, showing that the two standards don't agree with each other, or with the spectral metrics used in this study (**Figure 14C**).

We hypothesize that both methods may have significant degrees of error which may skew the hydration values. Previous work has shown that urine indices of hydration can lag behind systemic hydration²². This may be due to urine indices being indicative of all the urine in the bladder at the time the sample is taken, so it provides a value of hydration since the previous bladder void, not a snapshot of the person's hydration status at the time the sample is collected. In our studies, we did not control the time since last bladder void prior to collecting urine samples so this could have induced variability between the urine content in the bladder of each participant. Secondly, percent weight lost during an exercise period can fail to account for certain types of water loss, which can induce a degree of error on the metric. Weight lost during exercise is typically attributed solely to fluid lost as sweat during exercise but fails to take into account respiratory water loss, and weight changes due to carbohydrate or fat metabolism³⁶. While our studies' exercise regimens were generally short (between 25 minutes and one hour) and significant carbohydrate or fat metabolism should not have large effect on body weight during this duration, it is possible this contributed to the disagreement between standards. The sources of error identified in the use of two commonly used clinical standards could have affected the correlation between the chosen standards and the AUC of the water band. This indicates that different clinical standards, such as blood indices, should be explored in future studies to provide a more accurate picture of hydration status, and further reiterates the need for the development of a rapid, non-invasive hydration monitoring tool, such as a RS-based tool.

In an effort to further investigate the disagreement between the two standards chosen, we identified gender as a factor that could affect the accuracy of the standards. Literature has identified differences in the dehydration dynamics of females and males including significant differences in uSG, urine color, and body mass change when pair-matched according to exercise time and BMI, significantly higher sweat rates in males, and a delay in time to start sweating in females^{105,107,108}. It is hypothesized that these differences may have a multifactorial cause. Females have been shown to have more surface area per unit mass than males¹⁰⁷. Hormonal variations throughout the menstrual cycle may induce changes in systemic hydration and may

affect the degree of water loss during exercise¹⁰⁶. Females may have naturally lower water content than males, and at the same weight, have more body fat than males¹⁰⁴. In correlation with these known or hypothesized differences, we identified significant differences between the spectral responses and standards in relation to hydration in our studies. When separating the clinical standards into female and male groups we saw a significant difference ($p < 0.001$) in the variance and distribution of the male group's percent weight lost compared to the female group (**Figure 15A**). The percent weight loss of the male group was tightly clustered with a range of 0.363, while the female group had a range of 1.497. Additionally, the male group had a lower coefficient of variation (the ratio of the standard deviation to the mean) of 25.72% compared to the female group's coefficient of variation of 97.47%. We also identified a similar pattern of tighter distribution in the male group when the percent change AUC of the water band was analyzed by gender (**Figure 15B**). This indicates that despite the low correlation between the water band AUC and percent weight lost, the two metrics are clustering similarly, which is a promising result. Lastly, when the Pearson correlation was repeated on the gender-segregated values, an increase in the magnitude of all correlation coefficients was seen (**Figure 15C**). This highlights the importance of ensuring there are adequate numbers of both males and females in future hydration studies and may indicate that separate studies tailored to each gender group may be beneficial when developing this RS-based hydration monitoring method.

Study 3 considered various factors of importance discovered from Study 1 and 2 that have been discussed above, including a pre-study hydration protocol, ensuring all participants were routinely active thus adequately conditioned to perform the required exercise. This study also included collecting three repetitive measurements at each location to assess the homogeneity within each measurement location. Within two of the four participants who had repeated measurements conducted, there was a large degree of variability (**Figure 16A**). For example, the three measurements from one participant (P3) ranged from 1.7×10^6 to 2.3×10^6 a.u. (arbitrary units). The repetitive measurements were also a significant source of variability ($p < 0.05$) (**Figure 16B**). We hypothesize this variability could be stemming from two sources: physiological heterogeneity within the measurement location, and RS instrumentation variability. As discussed previously, the water content in fat is significantly lower than skin and muscle^{104,112,113}. If the probe was located where there was high heterogeneity of the composition of the underlying tissue at that location, this could induce a high degree of variability between the repetitive measurements. On the instrumentation side, previous research in our group has shown that changes in the orientation of the probe and pressure applied on the probe can impact the resulting spectra¹⁰¹. This could also indicate that a single measurement may not be sufficient to capture accurate hydration status information and future studies should investigate the use of continually acquired spectra throughout the exercise regimen. Regardless of the high inter-measurement variability seen in some participants, significant difference ($p < 0.05$) between

the pre-exercise and post-exercise percent change of the water band AUC was seen in half of the participants (**Figure 16C**). The pre-exercise hydration levels, as represented by pre-exercise uSG values below 1.01, may serve to decrease inter-subject variability and ensure that all participants will dehydrate similarly. Additionally, this exercise regimen slightly increased the personalization of the exercise to the ability level of each participant by allowing the participants to run at a comfortable pace, as long as they completed the 10 km run in one hour. Finally, this study also only recruited participants who were routinely active during the week with an average exercise per week of three days. More pronounced changes are expected with future studies as further standardization is incorporated.

Throughout this work, RS has been utilized to non-invasively detect changes in systemic hydration. After determining that the AUC of the water band and water to CH ratio can show water content, three *in vivo* studies were conducted to investigate the relationship between these spectral metrics and systemic hydration. A negative percent change, indicating a decrease in hydration after exercise, was found in the majority of participants results yet the magnitude of change varied. Additionally, a few percent change values were identified to be positive, indicating the opposite trend as expected. The RS-based measurements were impacted by a number of factors including large inter-subject variability and disagreement between commonly used hydration assessment methods. Future work must take these factors into consideration including conducting additional highly standardized studies, examining other commonly used hydration monitoring techniques, and ensuring adequate numbers of males and females in each study. Despite these factors, RS shows great promise for systemic hydration monitoring that is both rapid and non-invasive.

Conclusion

In summary, RS has shown feasibility for non-invasively detecting systemic hydration in exercising individuals. Gelatin-based tissue mimicking phantoms have been utilized to validate the relationship between water content and two spectral metrics, the AUC of the water band and the water to CH ratio. These metrics were then calculated from spectra collected from study participants before and after following an exercise regimen and their relationship to systemic hydration has been explored. Despite physiological differences between the four locations tested, no significant differences in variance were identified between the locations, highlighting the potential implementation of this tool at various locations. Multiple sources of variability have been identified including significant inter-subject and repetitive measurement variability, and these sources of variability must be taken into consideration for future studies. The advancement of RS for hydration monitoring has the potential to make inter-activity hydration monitoring a reality, thereby reducing the incidence of the negative side effects of dehydration and avoiding dangerous dehydration scenarios.

CHAPTER 3: CONCLUSIONS AND FUTURE DIRECTIONS

In summary, this work is the first demonstration of non-invasive hydration monitoring using RS. First, gelatin-based tissue mimicking phantoms were created with water content ranging from 65-90% to determine the optimal spectral metrics for assessing hydration information. Various exercise protocols, including unstandardized exercise, moderate exercise, and intensive exercise, were performed to determine the relationship between spectral metrics and systemic hydration. From the moderate exercise protocol, a trend in decreasing AUC of the water band following exercise was identified but the magnitude of change was highly variable. Through analysis of the sources of variability, we observed that significant inter-subject variation and variation based on gender had significant impact on our studies. We also identified a failure of the two clinical standards used, uSG and body weight lost, to accurately describe hydration status, thus making it difficult to benchmark this RS-based technique. Further standardization and intensive exercise in Study 3 resulted in significant decreases of the water band AUC following exercise, but also revealed significant variations in repetitive measurements. This RS-based technique has shown feasibility for non-invasive hydration monitoring, its increased ease of hydration monitoring can aid in the reduction of the negative side effect associated with dehydration. This work has the potential to benefit numerous populations including military personnel, athletes, laborers, the elderly, and children.

Future Directions

Various studies can be designed to address the main questions remaining following this work. First, more rigorous exercise protocols, such as running for up to 2 hours, need to be utilized to maximize the participants' water loss to ensure a large degree of change that the RS-based technique can measure. Furthermore, studies tailored to each gender should be performed to assess the performance of RS-based hydration monitoring in each gender. Additional considerations are required for a female-focused study including birth control use and type, and menstrual cycle phase, as these factors may play a role in hydration dynamics. Studies should also be performed to assess the sensitivity of RS for hydration monitoring by determining the minimum change that can be detected. Following the determination of the sensitivity of the technique, studies on military personnel should be performed as this is the target population this technique is currently being developed for. In future studies, additional analysis of other clinical standards should be considered, as the two standards utilized in this work fail to show accurate hydration status. Clinical standards such as bioelectric impedance, saliva osmolality, and blood osmolality should be investigated toward the benchmarking of this developed RS-based technique. Work could also be performed to increase the robustness of the standards used here including standardizing the time since last bladder void to try to increase the accuracy of the urine measurement.

REFERENCES

1. Lang, F. & Waldegger, S. Regulating cell volume. *Am Sci* **85**, 456–463 (1997).
2. Ritz, P. & Berrut, G. The importance of good hydration for day-to-day health. *Nutr Rev* **63**, S6–S13 (2005).
3. Häussinger, D. The role of cellular hydration in the regulation of cell function. *Biochemical Journal* **313**, 697 (1996).
4. Jéquier, E. & Constant, F. Water as an essential nutrient: the physiological basis of hydration. *European Journal of Clinical Nutrition* 2010 64:2 **64**, 115–123 (2009).
5. Armstrong, L. E. Hydration assessment techniques. *Nutr Rev* **63**, 40–54 (2005).
6. Thomas, D. R. *et al.* Understanding clinical dehydration and its treatment. *J Am Med Dir Assoc* **9**, 292–301 (2008).
7. Sawka, M. N., Latzka, W. A., Matott, R. P. & Montain, I. Dehydration and exercise performance hydration effects on temperature regulation. *Int. J. Sports Med* 108–110 (1998).
8. Gonzalez-Alonso, J., Mora-Rodriguez, R., Below, P. R. & Coyle, E. F. Dehydration reduces cardiac output and increases systemic and cutaneous vascular resistance during exercise. *J Appl Physiol* **79**, 1487–1496 (1995).
9. Popkin, B. M., D’anci, K. E. & Rosenberg, I. H. Water, hydration and health. *Nutr Rev* (2010) doi:10.1111/j.1753-4887.2010.00304.x.
10. Leiper, J. B. Intestinal water absorption - Implications for the formulation of rehydration solutions. *Int J Sports Med* **19**, S129–S132 (1998).
11. Arnaud, M. J. Mild dehydration: a risk factor of constipation? *European Journal of Clinical Nutrition* 2003 57:2 **57**, S88–S95 (2003).
12. El-Sharkawy, A. M., Sahota, O. & Lobo, D. N. Acute and chronic effects of hydration status on health. *Nutr Rev* **73**, 97–109 (2015).
13. Williams, S., Krueger, N., Davids, M., Kraus, D. & Kersch, M. Effect of fluid intake on skin physiology: distinct differences between drinking mineral water and tap water. *Int J Cosmet Sci* **29**, 131–138 (2007).
14. Mac-Mary, S. *et al.* Assessment of effects of an additional dietary natural mineral water uptake on skin hydration in healthy subjects by dynamic barrier function measurements and clinic scoring. *Skin Research and Technology* **12**, 199–205 (2006).
15. Wilson, M. M. G. & Morley, J. E. Impaired cognitive function and mental performance in mild dehydration. *European Journal of Clinical Nutrition* 2003 57:2 **57**, S24–S29 (2003).
16. Cohen, S. After effects of stress on human performance during a heat acclimatization regimen. *Aviation Space Environmental Medicine* 709–713 (1983).

17. Neelon, V. & Champagne, M. Managing cognitive impairment: The current bases for practice. *Key Aspects of Eldercare: Managing falls, incontinence and cognitive impairment*. 122–131 (1992).
18. Judelson, D. A. *et al.* Effect of hydration state on strength, power, and resistance exercise performance. *Med Sci Sports Exerc* **39**, 1817–1824 (2007).
19. Cheuvront, S. N., Carter, R. & Sawka, M. N. Fluid balance and endurance exercise performance. *Curr Sports Med Rep* **2**, 202–208 (2003).
20. Armstrong, L. E., Johnson, E. C. & Bergeron, M. F. COUNTERVIEW: Is drinking to thirst adequate to appropriately maintain hydration status during prolonged endurance exercise? No. *Wilderness Environ Med* **27**, 195–198 (2016).
21. Cian, C. *et al.* Influences of variations in body hydration on cognitive function: Effect of hyperhydration, heat stress, and exercise-induced dehydration. - PsycNET. *J Psychophysiol* **14**, 29–36 (2000).
22. Popowski, L. A. *et al.* Blood and urinary measures of hydration status during progressive acute dehydration. *Med Sci Sports Exerc* **33**, 747–753 (2001).
23. Neave, N. *et al.* Water ingestion improves subjective alertness, but has no effect on cognitive performance in dehydrated healthy young volunteers. *Appetite* **37**, 255–256 (2001).
24. Rogers, P. J., Kainth, A. & Stair, H. J. A drink of water can improve or impair mental performance depending on small differences in thirst. *Appetite* **36**, 57–58 (2001).
25. Szinnai, G., Schachinger, H., Arnaud, M. J., Linder, L. & Keller, U. Effect of water deprivation on cognitive-motor performance in healthy men and women. *Am J Physiol Regul Integr Comp Physiol* **289**, 275–280 (2005).
26. Baker, L. B., Conroy, D. E. & Kenney, W. L. Dehydration impairs vigilance-related attention in male basketball players. *Med Sci Sports Exerc* **39**, 976–983 (2007).
27. Bates, G. P. & Schneider, J. Hydration status and physiological workload of UAE construction workers: A prospective longitudinal observational study. *Journal of Occupational Medicine and Toxicology* **3**, 1–10 (2008).
28. Brake, D. J. & Bates, G. P. Fluid losses and hydration status of industrial workers under thermal stress working extended shifts. *Occup Environ Med* **60**, 90–96 (2003).
29. Miller, V. & Bates, G. Hydration of outdoor workers in north-west Australia. *J Occup Health Safety-Aust NZ* **23**, 79–87 (2007).
30. Bates, G. P., Miller, V. S. & Joubert, D. M. Hydration status of expatriate manual workers during summer in the Middle East. *Ann. Occup. Hyg* **54**, 137–143 (2010).
31. Garrett, D. C. *et al.* Engineering approaches to assessing hydration status. *IEEE Rev Biomed Eng* **11**, 233–248 (2018).
32. Armstrong, L. E. Assessing hydration status: the elusive gold standard. *J Am Coll Nutr* **26**, 575S–584S (2007).

33. Kehayias, J. & Valtuena, S. Neutron activation analysis determination of body composition... : Current Opinion in Clinical Nutrition & Metabolic Care. *Curr Opin Clin Nutr Metab Care* **2**, 453–463 (1999).
34. Shirreffs, S. M. Markers of hydration status. *European Journal of Clinical Nutrition* 2003 57:2 **57**, S6–S9 (2003).
35. Shirreffs, S. Markers of hydration status. *Journal of Sports Medicine and Physical Fitness* **40**, 80–84 (2000).
36. Maughan, R. J., Shirreffs, S. M. & Leiper, J. B. Errors in the estimation of hydration status from changes in body mass. <https://doi.org/10.1080/02640410600875143> **25**, 797–804 (2007).
37. Villiger, M. *et al.* Evaluation and review of body fluids saliva, sweat and tear compared to biochemical hydration assessment markers within blood and urine. *European Journal of Clinical Nutrition* 2018 72:1 **72**, 69–76 (2017).
38. De Buys Roessingh, A. S., Drukker, A. & Guignard, J.-P. Dipstick measurements of urine specific gravity are unreliable. doi:10.1136/adc.85.2.155.
39. Muñoz, C. X. *et al.* Assessment of hydration biomarkers including salivary osmolality during passive and active dehydration. *European Journal of Clinical Nutrition* 2013 67:12 **67**, 1257–1263 (2013).
40. Oppliger, R. A. & Bartok, C. Hydration testing of athletes. *Sports Medicine* 2002 32:15 **32**, 959–971 (2012).
41. Chevront, S. N., Kenefick, R. W. & Zambraski, E. J. Spot urine concentrations should not be used for hydration assessment: A methodology review. *Int J Sport Nutr Exerc Metab* **25**, 293–297 (2015).
42. Walsh, N. *et al.* Saliva parameters as potential indices of hydration status during acute dehydration. *Med Sci Sports Exerc* (2004) doi:10.1249/01.MSS.0000139797.26760.06.
43. Walsh, N. P., Montague, J. C., Callow, N. & Rowlands, A. V. Saliva flow rate, total protein concentration and osmolality as potential markers of whole body hydration status during progressive acute dehydration in humans. *Arch Oral Biol* **49**, 149–154 (2004).
44. Muñoz, C. X. *et al.* Assessment of hydration biomarkers including salivary osmolality during passive and active dehydration. *European Journal of Clinical Nutrition* 2013 67:12 **67**, 1257–1263 (2013).
45. Ely, A. R., Chevront, S. N., Kenefick, R. W. & Sawka, M. N. Limitations of salivary osmolality as a marker of hydration status. *Med. Sci. Sports Exerc* **43**, 1080–1084 (2011).
46. Taylor, N. A. S. *et al.* Observations on saliva osmolality during progressive dehydration and partial rehydration. *Eur J Appl Physiol* **112**, 3227–3237 (2012).
47. Morgan, R. M., Patterson, M. J. & Nimmo, M. A. Acute effects of dehydration on sweat composition in men during prolonged exercise in the heat. *Acta Physiol Scand* **182**, 37–43 (2004).
48. Fortes, M. *et al.* Tear fluid osmolality as a potential marker of hydration status. *Med. Sci. Sports Exerc* (2011) doi:10.1249/MSS.0b013e31820e7cb6.

49. Ungaro, C. T. *et al.* Non-invasive estimation of hydration status changes through tear fluid osmolarity during exercise and post-exercise rehydration. *Eur J Appl Physiol* **115**, 1165–1175 (2015).
50. Van Loan, M. D., Kopp, L. E., King, J. C., Wong, W. W. & Mayclin, P. L. Fluid changes during pregnancy: use of bioimpedance spectroscopy. <https://doi.org/10.1152/jappl.1995.78.3.1037> **78**, 1037–1042 (1995).
51. Thomas, B. J., Ward, L. C. & Cornish, B. H. Bioimpedance spectrometry in the determination of body water compartments: Accuracy and clinical significance. *Applied Radiation and Isotopes* **49**, 447–455 (1998).
52. Liang, M., Su, H. & Lee, N. Skin temperature and skin blood flow affect bioelectric impedance study of female fat-free mass. *Med Sci Sports Exerc* **32**, 221 (2000).
53. Bioelectrical impedance analysis in body composition measurement: National Institutes of Health Technology Assessment Conference Statement. *Am J Clin Nutr* **64**, (1996).
54. O'Brien, C., Young, A. J. & Sawka, M. N. Bioelectrical impedance to estimate changes in hydration status. *Int J Sports Med* **23**, 361–366 (2002).
55. Ozana, N. *et al.* Improved noncontact optical sensor for detection of glucose concentration and indication of dehydration level. *Biomedical Optics Express*, Vol. 5, Issue 6, pp. 1926-1940 **5**, 1926–1940 (2014).
56. Moran, D. *et al.* Hydration status measurement by radio frequency absorptiometry in young athletes-a new method and preliminary results. *Physiol Meas* (2004) doi:10.1088/0967-3334/25/1/005.
57. Reeder, J. T. *et al.* Resettable skin interfaced microfluidic sweat collection devices with chemesthetic hydration feedback. *Nature Communications* 2019 10:1 **10**, 1–12 (2019).
58. Sarvazyan, A. P., Tsyuryupa, S. N., Calhoun, M. & Utter, A. Acoustical method of whole-body hydration status monitoring. *Acoust Phys* **62**, 514 (2016).
59. Roy, S. C., Kissel, L. & Pratt, R. H. Elastic scattering of photons. *Radiation Physics and Chemistry* **56**, 3–26 (1999).
60. Liu, K., Zhao, Q., Li, B. & Zhao, X. Raman spectroscopy: A novel technology for gastric cancer diagnosis. *Front Bioeng Biotechnol* **10**, 354 (2022).
61. Jones, R. R., Hooper, D. C., Zhang, L., Wolverson, D. & Valev, V. K. Raman techniques: fundamentals and frontiers. *Nanoscale Research Letters* vol. 14 Preprint at <https://doi.org/10.1186/s11671-019-3039-2> (2019).
62. Movasaghi, Z., Rehman, S. & Rehman, I. U. Raman spectroscopy of biological tissues. *Appl Spectrosc Rev* **42**, 493–541 (2007).
63. Bergholt, M. S., Serio, A. & Albro, M. B. Raman spectroscopy: guiding light for the extracellular matrix. *Front Bioeng Biotechnol* **7**, 1–16 (2019).
64. Alinovi, M. *et al.* Applicability of confocal Raman microscopy to observe microstructural modifications of cream cheeses as influenced by freezing. *Foods* **9**, 679 (2020).

65. Masson, L. E. *et al.* Dual excitation wavelength system for combined fingerprint and high wavenumber Raman spectroscopy. *Analyst* **143**, 6049–6060 (2018).
66. Wolthuis, R. *et al.* Determination of water concentration in brain tissue by Raman spectroscopy. *Anal Chem* **73**, 3915–3920 (2001).
67. Ghita, A., Hubbard, T., Matousek, P. & Stone, N. Noninvasive detection of differential water content inside biological samples using deep Raman spectroscopy. *Anal Chem* **92**, 9449–9453 (2020).
68. Barroso, E. M. *et al.* Raman spectroscopy for assessment of bone resection margins in mandibulectomy for oral cavity squamous cell carcinoma. *Eur J Cancer* **92**, 77–87 (2018).
69. Barroso, E. M. *et al.* Discrimination between oral cancer and healthy tissue based on water content determined by Raman spectroscopy. *Anal Chem* **87**, 2419–2426 (2015).
70. Unal, M. & Akkus, O. Raman spectral classification of mineral- and collagen-bound water's associations to elastic and post-yield mechanical properties of cortical bone. *Bone* **81**, 315–326 (2015).
71. Caspers, P. J., Lucassen, G. W., Carter, E. A., Bruining, H. A. & Puppels, G. J. In vivo confocal Raman microspectroscopy of the skin: noninvasive determination of molecular concentration profiles. *Journal of Investigative Dermatology* **116**, 434–442 (2001).
72. SCHOEN, E. J. Minimum urine total solute concentration in response to water loading in normal men. *J Appl Physiol* **10**, 267–270 (1957).
73. Bar-Or, O., Dotan, R., Inbar, O., Rotshtein, A. & Zonder, H. Voluntary hypohydration in 10- to 12-year-old boys. <https://doi.org/10.1152/jap.1980.48.1.104> **48**, 104–108 (1980).
74. D'Anci, K. E., Constant, F. & Rosenberg, I. H. Hydration and cognitive function in children. *Nutr Rev* **64**, 457–464 (2006).
75. Cian, C., Barraud, P. A., Melin, B. & Raphel, C. Effects of fluid ingestion on cognitive function after heat stress or exercise-induced dehydration. *International Journal of Psychophysiology* **42**, 243–251 (2001).
76. D'anci, K. E., Mahoney, C. R., Vibhakar, A., Kanter, J. H. & Taylor, H. A. Voluntary dehydration and cognitive performance in trained college athletes. <http://dx.doi.org/10.2466/pms.109.1.251-269> **109**, 251–269 (2009).
77. Suhr, J. A., Hall, J., Patterson, S. M. & Niinistö, R. T. The relation of hydration status to cognitive performance in healthy older adults. *International Journal of Psychophysiology* **53**, 121–125 (2004).
78. Chevront, S. N. & Kenefick, R. W. Dehydration: physiology, assessment, and performance effects. *Compr Physiol* **4**, 257–285 (2014).
79. Gopinathan, P. M., Pichan, G. & Sharma, V. M. Role of dehydration in heat stress-induced variations in mental performance. *Archives of Environmental Health: An International Journal* **43**, 15–17 (1988).

80. Kenefick, R. W. Drinking strategies: planned drinking versus drinking to thirst. *Sports Medicine* **48**, 31–37 (2018).
81. Bak, A., Tsiami, A. & Greene, C. Methods of assessment of hydration status and their usefulness in detecting dehydration in the elderly. *Current Research in Nutrition and Food Science* **5**, 43–54 (2017).
82. Rose, D. P. *et al.* Adhesive RFID sensor patch for monitoring of sweat electrolytes. *IEEE Trans Biomed Eng* **62**, 1457–1465 (2015).
83. De Guzman, K. & Morrin, A. Screen-printed Tattoo Sensor towards the Non-invasive Assessment of the Skin Barrier. *Electroanalysis* **29**, 188–196 (2017).
84. Sarvazyan, A., Tatarinov, A. & Sarvazyan, N. Ultrasonic assessment of tissue hydration status. *Ultrasonics* **43**, 661–671 (2005).
85. Sarvazyan, A. P., Tsyuryupa, S. N., Calhoun, M. & Utter, A. Acoustical method of whole-body hydration status monitoring. *Acoust Phys* **62**, 514 (2016).
86. Shavit, I., Brant, R., Nijssen-Jordan, C., Galbraith, R. & Johnson, D. W. A novel imaging technique to measure capillary-refill time: improving diagnostic accuracy for dehydration in young children With gastroenteritis. *Pediatrics* **118**, 2402–2408 (2006).
87. Koljenovic, S. *et al.* Tissue characterization using high wave number Raman spectroscopy. <https://doi.org/10.1117/1.1922307> **10**, 031116 (2005).
88. Krafft, C. & Popp, J. Raman4Clinics: the prospects of Raman-based methods for clinical application. *Analytical and Bioanalytical Chemistry* 2015 407:27 **407**, 8263–8264 (2015).
89. Smith, E. & Dent, G. *Modern Raman spectroscopy—a practical approach*. *Journal of Raman Spectroscopy* vol. 36 (John Wiley & Sons, Ltd, 2005).
90. Neugebauer, U., Rösch, P. & Popp, J. Raman spectroscopy towards clinical application: drug monitoring and pathogen identification. *Int J Antimicrob Agents* **46**, S35–S39 (2015).
91. Choe, C., Lademann, J. & Darvin, M. E. Depth profiles of hydrogen bound water molecule types and their relation to lipid and protein interaction in the human stratum corneum in vivo. *Analyst* **141**, 6329–6337 (2016).
92. Hu, Q., Ouyang, S., Li, J. & Cao, Z. Raman spectroscopic investigation on pure D₂O/H₂O from 303 to 573 K: interpretation and implications for water structure. *Journal of Raman Spectroscopy* **48**, 610–617 (2017).
93. Barroso, E. M. *et al.* Water concentration analysis by Raman spectroscopy to determine the location of the tumor border in oral cancer surgery. *Cancer Res* **76**, 5945–5953 (2016).
94. García-Flores, A. F. *et al.* High-wavenumber FT-Raman spectroscopy for in vivo and ex vivo measurements of breast cancer. *Theor Chem Acc* **130**, 1231–1238 (2011).
95. Hubbard, T. J. E., Dudgeon, A. P., Ferguson, D. J., Shore, A. C. & Stone, N. Utilization of Raman spectroscopy to identify breast cancer from the water content in surgical samples containing blue dye. *Transl Biophotonics* **3**, 1–8 (2021).

96. Casa, D. J. *et al.* National Athletic Trainers' Association Position Statement: Fluid Replacement for Athletes. *J Athl Train* **35**, 212–224 (2000).
97. MASSON, L. E. *et al.* In vivo Raman spectroscopy monitors cervical change during labor. *Am J Obstet Gynecol* (2022) doi:10.1016/J.AJOG.2022.02.019.
98. O'Brien, C. M. *et al.* Development of a visually guided Raman spectroscopy probe for cervical assessment during pregnancy. *J Biophotonics* **12**, e201800138 (2019).
99. O'Brien, C. M. *et al.* In vivo Raman spectroscopy for biochemical monitoring of the human cervix throughout pregnancy. *Am J Obstet Gynecol* **218**, 528.e1-528.e18 (2018).
100. Vargis, E. *et al.* Detecting biochemical changes in the rodent cervix during pregnancy using raman spectroscopy. *Ann Biomed Eng* **40**, 1814–1824 (2012).
101. Pence, I. J., Vargis, E. & Mahadevan-Jansen, A. Assessing variability of in vivo tissue Raman spectra. *Appl Spectrosc* **67**, 789–800 (2013).
102. Monroy, G. L. *et al.* Multimodal handheld probe for characterizing otitis media — integrating Raman spectroscopy and optical coherence tomography. *Frontiers in Photonics* **3**, (2022).
103. Lieber, C. A. & Mahadevan-Jansen, A. Automated method for subtraction of fluorescence from biological Raman spectra. *Applied Spectroscopy, Vol. 57, Issue 11, pp. 1363-1367* **57**, 1363–1367 (2003).
104. Ritz, P. *et al.* Influence of gender and body composition on hydration and body water spaces. *Clinical Nutrition* **27**, 740–746 (2008).
105. Armstrong, L. E., Johnson, E. C., McKenzie, A. L., Ellis, L. A. & Williamson, K. H. Endurance cyclist fluid intake, hydration status, thirst, and thermal sensations: gender differences. *Int J Sport Nutr Exerc Metab* **26**, 161–167 (2016).
106. Aula Médica España Ramos-Jiménez, G. *et al.* Gender-and hydration-associated differences in the physiological response to spinning. *Nutr Hosp* **29**, 644–651 (2014).
107. Hazelhurst, L. T. & Claassen, N. Gender differences in the sweat response during spinning exercise. *J Strength Cond Res* **20**, 723–724 (2006).
108. Grucza, R., Szczypaczewska, M. & Kozłowski, S. Thermoregulation in hyperhydrated men during physical exercise. *Eur J Appl Physiol Occup Physiol* **56**, 603–607 (1987).
109. Björntorp, P. Adipose tissue distribution and function. *Int J Obes* **15 Suppl 2**, 67–81 (1991).
110. Enzi, G. *et al.* Subcutaneous and visceral fat distribution according to sex, age, and overweight, evaluated by computed tomography. *Am J Clin Nutr* **44**, 739–746 (1986).
111. Deshayes, T. A., Jeker, D. & Goulet, E. D. B. Impact of pre-exercise hypohydration on aerobic exercise performance, peak oxygen consumption and oxygen consumption at lactate threshold: A systematic review with meta-analysis. *Sports Medicine* **50**, 581–596 (2020).
112. Lorenzo, I., Serra-Prat, M. & Carlos Yébenes, J. The role of water homeostasis in muscle function and frailty: a review. *Nutrients* **11**, (2019).

113. Yu, Z. *et al.* Assessment of skin properties in chronic lymphedema: measurement of skin stiffness, percentage water content, and transepidermal water loss. *Lymphat Res Biol* **18**, 212–218 (2020).
114. Smith, C. J. & Havenith, G. Body mapping of sweating patterns in male athletes in mild exercise-induced hyperthermia. *Eur J Appl Physiol* **111**, 1391–1404 (2011).
115. Coull, N. A., West, A. M., Hodder, S. G., Wheeler, P. & Havenith, G. Body mapping of regional sweat distribution in young and older males. *Eur J Appl Physiol* **121**, 109–125 (2021).
116. Olsen, L. O., Takiwaki, H. & Serup, J. High-frequency ultrasound characterization of normal skin. Skin thickness and echographic density of 22 anatomical sites. *Skin Research and Technology* **1**, 74–80 (1995).
117. Calbet, J. A. L. *et al.* Why do arms extract less oxygen than legs during exercise? *Am J Physiol Regul Integr Comp Physiol* **289**, 1448–1458 (2005).